

Supporting Information

**Light-Triggered Nitric Oxide (NO) Release from Photoresponsive  
Polymersomes for Corneal Wound Healing**

**Yutian Duan,<sup>†</sup> Yong Wang,<sup>‡</sup> Xiaohu Li,<sup>#</sup> Guozhen Zhang,<sup>†</sup> Guoying Zhang,<sup>†</sup> Jinming  
Hu<sup>†\*</sup>**

<sup>†</sup>*CAS Key Laboratory of Soft Matter Chemistry, Hefei National Laboratory for Physical  
Science at the Microscale, Department of Polymer Science and Engineering, University of  
Science and Technology of China, Hefei 230026, Anhui, China;*

<sup>‡</sup>*Department of Ophthalmology, The First Affiliated Hospital of Anhui Medical University,  
Hefei, Anhui 230022, China;*

<sup>#</sup>*Department of Radiology, The First Affiliated Hospital of Anhui Medical University, Hefei,  
Anhui 230022, China;*

<sup>†</sup>*Hefei National Laboratory for Physical Sciences at the Microscale, iChEM (Collaborative  
Innovation Center of Chemistry for Energy Materials), University of Science and Technology  
of China, Hefei, Anhui 230026, P. R. China*

To whom the correspondence should be addressed. E-mail: [jmhu@ustc.edu.cn](mailto:jmhu@ustc.edu.cn) (J.H.)

## Experimental Section

**Materials.** 4-Nitrobenzyl alcohol, 4-nitroaniline, aniline, 4-nitrophenyl isocyanate, doxorubicin hydrochloride (DOX), fluorescein disodium salt, and 2-nitrobenzaldehyde were purchased from Energy Chemical. Benzaldehyde, *o*-phenylenediamine, sodium borohydride (NaBH<sub>4</sub>), sodium nitrite (NaNO<sub>2</sub>), sodium sulfate anhydrous (Na<sub>2</sub>SO<sub>4</sub>), chloral hydrate, and dibutyltin dilaurate (DBTL) were purchased from Sinopharm Co., Ltd. 2-Isocyanatoethyl methacrylate, *N,N'*-bis(1-methylpropyl)-1,4-phenylenediamine, and Griess Reagent were purchased from Sigma-Aldrich. Coumarin 102 and Nile red were purchased from J&K Scientific Co., Ltd. 2,2'-Azobis(2-methylpropionitrile) (AIBN) was purified by recrystallization from 95% ethanol. All other chemicals were purchased from commercially available sources and were used as received unless otherwise indicated. Solvents were purified through a Pure Solv™ system. Water was deionized through a Milli-Q apparatus (Millipore) with a resistivity of 18.2 MΩ·cm. BNN-6<sup>1</sup> and poly(ethylene oxide) (PEO)-based macroRAFT agent<sup>2</sup> were synthesized according to reported procedures.

**Sample Synthesis.** Synthetic schemes employed for the preparation of 2-((((4-((2-nitrobenzyl)(nitroso)amino)benzyl)oxy)carbonyl)amino)ethyl methacrylate (*o*NBN), 2-((((4-((4-nitrobenzyl)(nitroso)amino)benzyl)oxy)carbonyl)amino)ethyl methacrylate (*p*NBN), and 2-((((4-(benzyl(nitroso)amino)benzyl)oxy)carbonyl)amino)ethyl methacrylate (BN) monomers are shown in Scheme 2. The preparation of PEO-*b*-P*o*NBN (**BP1**), PEO-*b*-P*p*NBN (**BP2**), and PEO-*b*-PBN (**BP3**) amphiphilic diblock copolymers through reversible addition-fragmentation chain transfer (RAFT) polymerization using PEO-based macroRAFT agent is shown in Scheme 2b.

*Synthesis of (2-((((4-((2-nitrobenzyl)(nitroso)amino)benzyl)oxy)carbonyl)amino)ethyl methacrylate) (oNBN, Scheme 2a).* 4-Nitrobenzyl alcohol (1.50 g, 9.79 mmol, 1.0 equiv.) and Pd/C (0.15 g, 0.1 equiv.) were dissolved in C<sub>2</sub>H<sub>5</sub>OH (20 mL) and stirred at room temperature in a hydrogen atmosphere. After 1.5 h, the reaction mixture was filtered and the filtrate was condensed under reduced pressure to obtain 4-aminobenzyl alcohol. Subsequently, 4-aminobenzyl alcohol (2.00 g, 16.24 mmol, 1.0 equiv.) and 2-nitrobenzaldehyde (2.45 g, 16.24 mmol, 1.0 equiv.) were dissolved in C<sub>2</sub>H<sub>5</sub>OH (60 mL) and stirred at room temperature overnight.

Then, the reaction mixture was filtered and the residue (2.00 g, 7.80 mmol, 1.0 equiv.) was diluted with THF (30 mL). Afterward, NaBH<sub>4</sub> (0.295 g, 7.80 mmol, 1.0 equiv.) was added and stirred at room temperature for 2 h. Then, water (5 mL) was added into the reaction mixture and THF was removed under reduced pressure. The residue was extracted with dichloromethane (DCM) and the organic phase was dried over anhydrous Na<sub>2</sub>SO<sub>4</sub>, yielding 4-((2-nitrobenzyl)amino)phenyl)methanol as orange oil.

Next, 4-((2-nitrobenzyl)amino)phenyl)methanol (1.03 g, 3.97 mmol, 1.0 equiv.) was dissolved in acetic acid (20 mL) and NaNO<sub>2</sub> (0.30 g, 4.41 mmol, 1.1 equiv.) aqueous solution (60 mL) was added dropwise. The mixture was stirred at room temperature for 20 min and was then poured into a saturated NaHCO<sub>3</sub> solution (Caution! CO<sub>2</sub> gas generation). The aqueous phase was extracted with DCM (60 mL × 5) and the combined organic phase was dried over Na<sub>2</sub>SO<sub>4</sub>. After removing DCM by a rotary evaporator, the residue was purified by column chromatography, yielding *N*-(4-(hydroxymethyl)phenyl)-*N*-(2-nitrobenzyl)nitrous amide as a light yellowish solid (0.73 g, yield: 64%). Next, *N*-(4-(hydroxymethyl)phenyl)-*N*-(2-nitrobenzyl)nitrous amide (0.73 g, 2.54 mmol, 1.0 equiv.), 2-isocyanatoethyl methacrylate (0.39 g, 2.54 mmol, 1.0 equiv.), and DBTL (11 μL) were dissolved in THF (20 mL) and were stirred at room temperature overnight. After removing the organic solvent, the solid residue was further purified by column chromatography, yielding *o*NBN monomer as yellowish solid (0.95 g, yield: 84.8%).

BN and *p*NBN monomers were synthesized using a similar protocol and the synthetic procedure is shown in Scheme 2a. During the preparation process, benzaldehyde or *p*-nitrobenzaldehyde was used to replace *o*-nitrobenzaldehyde as the starting material. In addition, *N*-(4-(hydroxymethyl)phenyl)-*N*-(2-methoxybenzyl)nitrous amide and *N*-(2-cyanobenzyl)-*N*-(4-(hydroxymethyl)phenyl)nitrous amide were synthesized using *o*-methoxybenzaldehyde and *o*-cyanobenzaldehyde to replace *o*-nitrobenzaldehyde. *N*-(2-nitrobenzyl)-*N*-phenylnitrous amide (**M1**) and *N*-benzyl-*N*-phenylnitrous amide (**M3**) control compounds were synthesized by nitrosation of *N*-(2-nitrobenzyl)-*N*-aniline (**M2**)<sup>3</sup> and *N*-benzyl-*N*-aniline (**M4**)<sup>4</sup>, respectively.

*Synthesis of 4-((2-nitrobenzyl)(nitroso)amino)benzyl (4-nitrophenyl)carbamate (NB(NO)A, Figure S16a).* *N*-(4-(hydroxymethyl)phenyl)-*N*-(2-nitrobenzyl)nitrous amide precursor (0.30 g,

1.04 mmol, 1.0 equiv.), 4-nitrophenyl isocyanate (0.17 g, 1.04 mmol, 1.0 equiv.), and DBTL (5  $\mu$ L) were dissolved in THF (20 mL), and were stirred at room temperature overnight. After removal of THF under vacuum, the reaction mixture was purified by column chromatography to obtain the named product (0.41 g, yield: 87.2%).

**Synthesis of PEO-*b*-P*o*NBN Amphiphiles (Scheme 2b).** Typically, *o*NBN monomer (442 mg, 1.00 mmol, 50.0 equiv.), PEO-based macroRAFT agent (45 mg, 0.02 mmol, 1.0 equiv.), and AIBN (0.33 mg, 0.002 mmol, 0.1 equiv.) were dissolved in DMSO (0.7 mL) and were added into a sealed tube. The tube was degassed by three freeze–pump–thaw cycles and then sealed under vacuum. After stirring at 70 °C for 8 h, the polymerization reaction was quenched by immersing the reaction tube into liquid nitrogen. The tube was then opened, exposed to air, diluted with DCM, and precipitated into an excess of diethyl ether. The above dissolution-precipitation cycle was repeated three times. The precipitate was then collected by filtration and was dried in a vacuum oven overnight at room temperature, affording a yellowish solid (120 mg, yield: 24.6%). The degree of polymerization (DP) of the P*o*NBN block was calculated to be  $\sim$ 25 by  $^1\text{H}$  NMR analysis (Table S1 and Figure S18a); thus, the diblock copolymer was denoted as PEO<sub>45</sub>-*b*-P*o*NBN<sub>25</sub> (**BP1**, Table S1).

To prepare the PEO-*b*-P*p*NBN (**BP2**) and PEO-*b*-PBN (**BP3**) diblock copolymers, *p*NBN and BN monomers were used instead of *o*NBN. The structural parameters of the synthesized PEO<sub>45</sub>-*b*-P*p*NBN<sub>30</sub> (**BP2**) and PEO<sub>45</sub>-*b*-PBN<sub>46</sub> (**BP3**) are summarized in Table S1.

**Self-Assembly of PEO-*b*-P*o*NBN Amphiphiles.** 5 mg of **BP1** was dissolved in 1,4-dioxane (1 mL), and the solution was stirred at 25 °C for 30 min. Then, 0.5 mL of pure water was slowly added at 1 mL/h via a syringe pump. The mixture was then extruded through a syringe filter (220 nm) four times. After that, pure water (2.5 mL) was then injected to frozen the assemblies at a rate of 1 mL/h. 1,4-Dioxane was removed by dialysis (MWCO 3.0 kDa) against pure water or PBS buffer solution (pH 7.4, 10 mM). For the self-assembly of **BP2** diblock copolymers, 1 mg of **BP2** was dissolved in 1,4-dioxane (1 mL), and the solution was stirred at 25 °C for 30 min. Then, 9 mL of deionized water was injected at a rate of 1 mL/h using a syringe pump. After the water addition, the organic solvent (i.e., 1,4-dioxane) was removed by dialysis (MWCO 3.0 kDa) against deionized water.

**Preparation of DOX-Loaded BP1 Vesicles.** 5 mg of **BP1** was dissolved in 1,4-dioxane (1 mL), and the solution was stirred at 25 °C for 30 min. Then, 0.5 mL of DOX·HCl aqueous solution (20 mg/mL) was slowly added at 1 mL/h via a syringe pump. After addition, the mixture was extruded through a syringe filter (220 nm) four times. After that, 1.5 mL of DOX·HCl aqueous solution (20 mg/mL) was added within 1.5 h. Afterward, 1,4-dioxane and unloaded DOX·HCl were removed by dialysis (MWCO 3.0 kDa) against deionized water. In a similar protocol, Nile red (NR)-loaded vesicles were also prepared and the unloaded NR was removed by exhaustive dialysis against deionized water.

**Light-Triggered Release of DOX.** 400 µL of the as-prepared DOX-loaded **BP1** vesicles without or with 365 nm irradiation was dialyzed against 10 mL of pure deionized water. At predetermined time points, the dialysate was replaced with 10 mL of fresh deionized water. The dialysate was subjected to lyophilization and the solid residues were re-dissolved in 1 mL of DMSO/H<sub>2</sub>O (v/v = 3/1). The DOX concentration was determined by fluorescence spectroscopy against a standard calibration curve. To establish a standard calibration curve of DOX, a series of DOX solutions (0.078125 nM - 10 µM) in DMSO/H<sub>2</sub>O (v/v = 3/1) were prepared and the corresponding fluorescence spectroscopy was measured. The excitation and emission wavelengths were set at 480 nm and 593 nm, respectively.

**In Vitro Cytotoxicity Assay.** Cell viability was examined by the Alamar blue assay. Briefly, human corneal epithelial cells (HCECs) were seeded in a 96-well plate at an initial density of 10,000 cells/well in 100 µL of DMEM complete medium. After incubation for 24 h, the culture medium was removed. **BP1** vesicles were diluted with DMEM complete medium or PBS buffer (pH 7.4, 10 mM), and then 100 µL of mixture solutions were added to 96-well plate to achieve different polymersomes concentrations (0.4, 0.2, 0.1, 0.05, 0.02, 0.01 g/L). After incubation for 4 h, the mixture solutions were removed and the 96-well plate was rinsed with 100 µL of PBS three times. Afterward, the plate was irradiated with a hand-held UV lamp for varying times (e.g., 0, 5, 10, or 20 min). After irradiation, the PBS in each well was removed and was replaced by 100 µL of DMEM complete medium. The cells were incubated for another 24, 48, 72, and 88 h and Alamar blue reagent (10 µL, Thermo Fisher) was added to each well. After the addition, the cells were further incubated with 5% CO<sub>2</sub> for 4 h at 37 °C. The fluorescence emission at

590 nm was recorded on a microplate reader using 550 nm as the excitation wavelength. The cell viability was calculated using the following equation:

$$\text{Cell viability (\%)} = (\text{FL}_{\text{sample}} - \text{FL}_{\text{blank}}) / (\text{FL}_{\text{control}} - \text{FL}_{\text{blank}}) \times 100\%$$

Where  $\text{FL}_{\text{sample}}$  is the fluorescence intensity of the solution in the well in which the cells were treated with **BP1** vesicles;  $\text{FL}_{\text{blank}}$  is the fluorescence intensity of the cell culture medium without cells; and  $\text{FL}_{\text{control}}$  is the fluorescence intensity of the solution in the well in which the cells were treated with the DMEM medium without **BP1** vesicles.

***Determination of NO Contents Using Griess Assay.*** 3 mL of **BP1** vesicle dispersion or NO-releasing precursors (40  $\mu\text{M}$ ) were placed in a standard quartz cuvette. The sample was irradiated with a hand-held UV lamp (365 nm, 4  $\text{mW}/\text{cm}^2$ ) and an aliquot sample (150  $\mu\text{L}$ ) was periodically withdrawn at predetermined time points. The irradiated sample was mixed with an equal volume of Griess reagent (Sigma-Aldrich, product number: 03553) and was incubated at room temperature under dark condition for 10 min. The nitrite concentration was determined by UV-vis spectroscopy based on the absorbance intensity at 526 nm against a standard calibration curve.

***In vitro Scratch Assay.*** Human corneal epithelial cells (HCECs) were seeded in a 96-well plate at an initial density of  $6 \times 10^4$  cells/well in 100  $\mu\text{L}$  of DMEM complete medium. After a confluent monolayer was formed, the culture medium was removed. The cell monolayers were scraped with a p200 pipet tip to form a straight line.<sup>5</sup> The debris was removed by carefully washing the cells with PBS. Next, **BP1** vesicles (the final concentration was fixed at 0.1  $\text{mg}/\text{mL}$ ) or PBS (pH 7.4, 10 mM) or GSNO was added and the cells were further incubated for 4 h. Afterward, 100  $\mu\text{L}$  of DMEM complete medium was added and the cells after coincubation with **BP1** vesicles were irradiated with a hand-held UV lamp for 0 min, 5 min, or 10 min, respectively. The plates were further incubated at 37  $^{\circ}\text{C}$  and the cells were imaged on a phase-contrast microscope at a predetermined time.

***Photo-Mediated Intracellular NO Release Observed by Confocal Laser Scanning Microscopy (CLSM).*** Briefly, HeLa cells were seeded in a 4-well plate at an initial density of 150,000 cells/well in 500  $\mu\text{L}$  of DMEM complete medium. After incubation for 8 h, the culture medium was removed and **BP1** vesicles (0.4  $\text{g}/\text{L}$ , 500  $\mu\text{L}$ ) in DMEM complete medium was

added; the cells were further incubated for 8 h prior to the addition of pyronine probe (0.1 mM). After 30 min incubation, the cells were irradiated with or without 365 nm hand-held UV lamp for 20 min. Then, the culture medium was removed and rinsed with PBS buffer. The cells were imaged by CLSM. The excitation wavelength was set at 514 nm and the red channel was set at 580-630 nm.

***In vivo* Cornea Wound Healing.** Six-week-old male Sprague-Dawley (SD) rats with an average body weight of 250 g were purchased from the Central Laboratory Animal Inc. (China). All animal experiments were approved by the Institutional Animal Care and Use Committee of the University of Science and Technology of China (USTC). The corneal wound healing experiments were conducted under the Association for Research in Vision and Ophthalmology (ARVO) statement. The mice were first anesthetized (0.4 mL/kg) by a chloral solution (0.1 g/mL). The corneal epithelial cells were removed by a surgical blade to create corneal wounds.<sup>6</sup> Wounded corneas were randomly assigned to receive different treatments: PBS buffer, **BP1** vesicles (1.25 mg/mL, ~1.43 mM NO) without light irradiation, **BP1** vesicles (1.25 mg/mL, ~1.43 mM NO) with prior light irradiation for 20 min, and GSNO solution (1.43 mM). For each treatment, 20  $\mu$ L of PBS or vesicle solutions or GSNO was added topically to the wound corneas. Each treatment group consisted of four corneas and the treatment was implemented every 8 hour. The corneal epithelial defects were recorded by a 0.5% fluorescein sodium solution at predetermined times. The stained corneas were imaged by a hand-held Dino-Lite digital microscope (AM5218MZT) and the wound areas were analyzed by calculation of the stained areas using ImageJ software.

### **Characterization.**

Nuclear magnetic resonance (NMR) spectra were recorded on a Bruker AV300 NMR (300 MHz) spectrometer operated in the Fourier transform mode. Deuterated chloroform ( $\text{CDCl}_3$ ) and dimethyl sulfone ( $\text{DMSO-}d_6$ ) were used as the solvents. Molecular weights and molecular weight distributions were determined by gel permeation chromatography (GPC) equipped with Waters 1515 pump and Waters 2414 differential refractive index detector (set at 30 °C). It used a series of two linear Styragel columns (HR2 and HR4) at an oven temperature of 45 °C. The eluent was THF at a flow rate of 1.0 mL/min. A series of polystyrene standards with low

polydispersities were employed for calibration. UV/Vis spectra were recorded on a TU-1910 double-beam UV-vis spectrophotometer (Puxi General Instrumental Company, China). Fluorescence spectra were performed on an F-4600 (Hitachi) spectrofluorometer. Dynamic laser light scattering (LLS) measurements were conducted on a Zetasizer Nano ZS (Malvern). The scattered light was collected at a fixed angle of 173° for the duration of ~5 min. All data were averaged over three consecutive measurements. Electron paramagnetic resonance (EPR) spectroscopy was recorded on a JES-FA200 (JEOL) spectrometer. The measurements were conducted at room temperature and the following parameters were used: modulation frequency: 100 kHz; modulation amplitude: 0.35 mT; scanning field: 324.3 ± 5 mT; microwave power: 1 mW; microwave frequency: 9.063 GHz. Transmission electron microscopy (TEM) observations were performed on a JEM-2100 electron microscope (JEOL Ltd.) at an acceleration voltage of 200 kV. TEM samples were prepared by placing 20 μL of aqueous dispersions (0.1 g/L) of assembled aggregates on copper grids coated with thin films of Formvar and carbon successively.

### Statistical Analysis

The results are expressed as mean ± standard deviation (s.d.). Standard deviation is indicated by the error bars. The *p* values were calculated using Student's t-test and *p* < 0.05 was considered statistically significant.

### References

- (1) Fan, J.; He, N. Y.; He, Q. J.; Liu, Y.; Ma, Y.; Fu, X.; Liu, Y. J.; Huang, P.; Chen, X. Y., A novel self-assembled sandwich nanomedicine for NIR-responsive release of NO. *Nanoscale* **2015**, *7*, 20055-20062.
- (2) Rieger, J.; Stoffelbach, F.; Bui, C.; Alaimo, D.; Jerome, C.; Charleux, B., Amphiphilic poly(ethylene oxide) macromolecular RAFT agent as a stabilizer and control agent in ab initio batch emulsion polymerization. *Macromolecules* **2008**, *41*, 4065-4068.
- (3) Glotz, G.; Lebl, R.; Dallinger, D.; Kappe, C. O., Integration of Bromine and Cyanogen Bromide Generators for the Continuous-Flow Synthesis of Cyclic Guanidines. *Angew. Chem. Int. Ed.* **2017**, *56*, 13786-13789.



- (4) Schonbauer, D.; Lukas, F.; Schnurch, M., Toluene and its Derivatives as Atom-Efficient Benzylating Agents for Secondary Amines. *Synlett* **2019**, *30*, 94-98.
- (5) Liang, C. C.; Park, A. Y.; Guan, J. L., In vitro scratch assay: a convenient and inexpensive method for analysis of cell migration in vitro. *Nat. Protoc.* **2007**, *2*, 329-333.
- (6) Choi, H. W.; Kim, J.; Kim, J.; Kim, Y.; Song, H. B.; Kim, J. H.; Kim, K.; Kim, W. J., Light-Induced Acid Generation on a Gatekeeper for Smart Nitric Oxide Delivery. *ACS Nano* **2016**, *10*, 4199-4208.

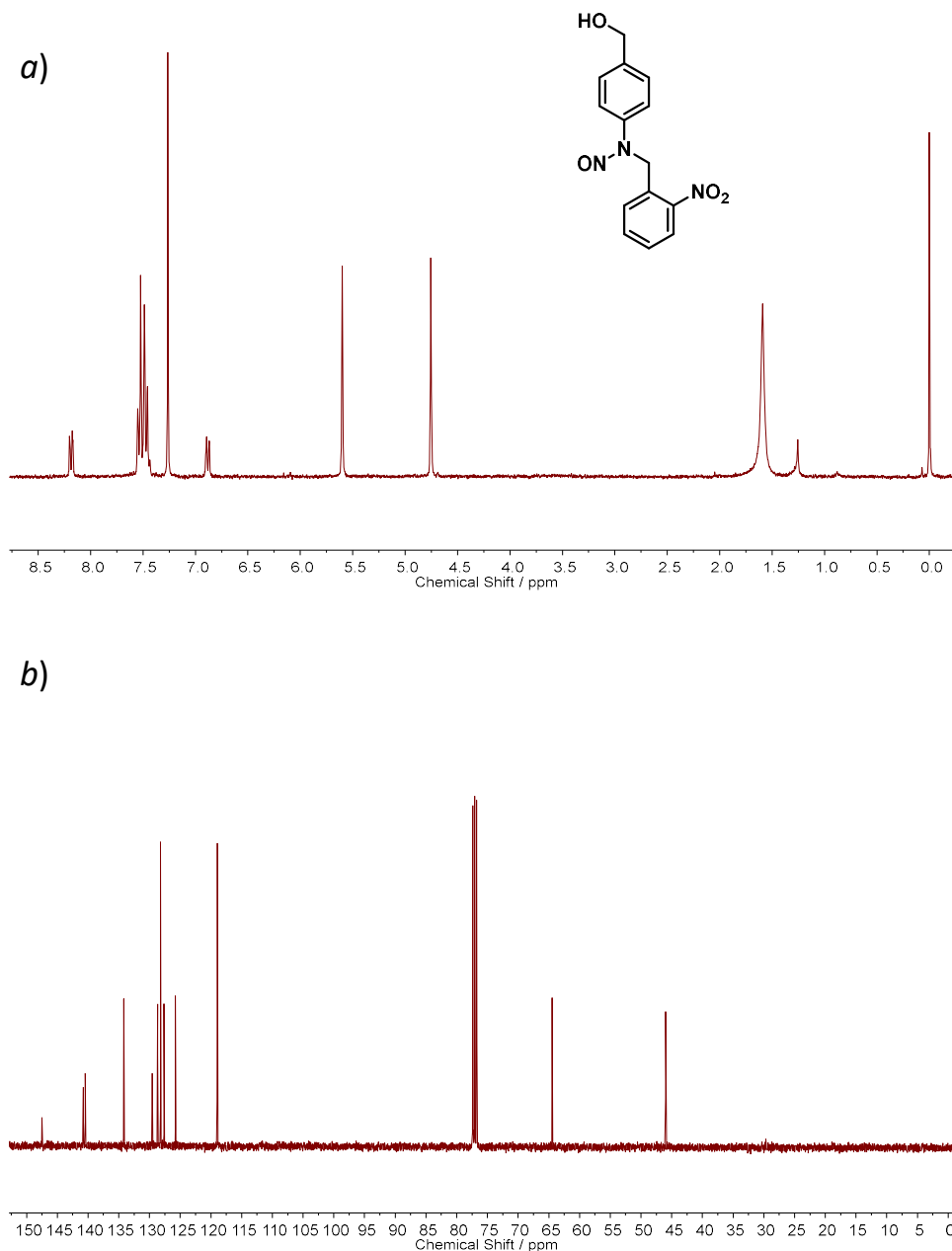


**Figure S1.** (a)  $^1\text{H}$  and (b)  $^{13}\text{C}$  NMR spectra recorded in  $\text{CDCl}_3$  for *N*-(4-(hydroxymethyl)phenyl)-*N*-(2-nitrobenzyl)nitrous amide.

$^1\text{H}$  NMR (300 MHz, Chloroform-*d*,  $\delta$ , ppm): 8.21 – 8.16 (m, 1H), 7.71 – 7.34 (m, 6H), 6.88 (d,  $J = 7.7$  Hz, 1H), 5.60 (s, 2H), 4.75 (s, 2H).

$^{13}\text{C}$  NMR (101 MHz, Chloroform-*d*,  $\delta$ , ppm): 147.50, 140.77, 140.45, 134.17, 129.57, 128.66, 128.21, 127.63, 125.79, 118.96, 64.45, 45.98.

ESI-MS:  $m/z$  calc. for  $\text{C}_{14}\text{H}_{13}\text{N}_3\text{O}_4\text{Na}^+$  310.0798, Found:  $[\text{M} + \text{Na}]^+ = 310.0804$ .

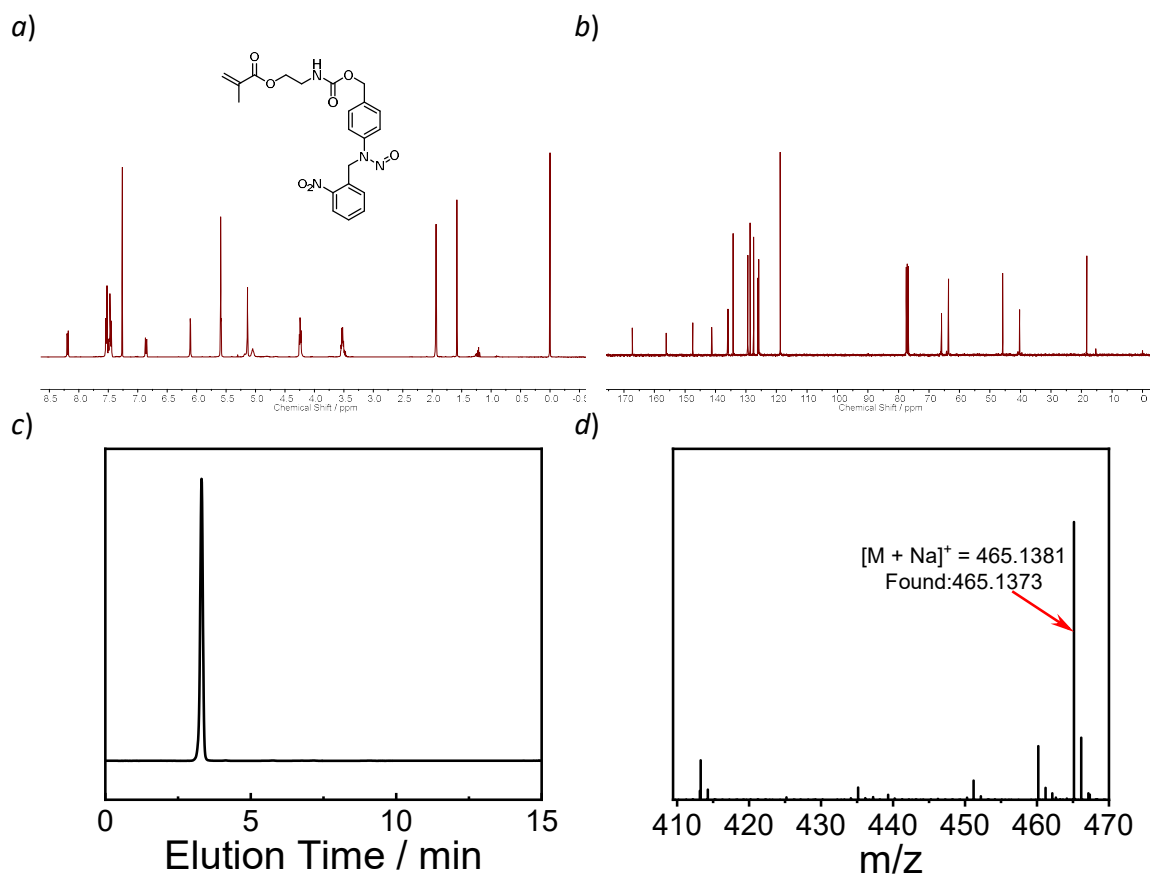


**Figure S2.** (a) <sup>1</sup>H and (b) <sup>13</sup>C NMR spectra recorded in CDCl<sub>3</sub> for *o*NBN monomer. (c) HPLC profile recorded at 258 nm for *o*NBN monomer (1 mM; CH<sub>3</sub>CN/H<sub>2</sub>O, v/v = 7/3 (0-3 min), 7/3-9/1 (3-15 min) as the eluent). (d) ESI mass spectrum recorded for *o*NBN monomer.

<sup>1</sup>H NMR (400 MHz, Chloroform-*d*, δ, ppm): 8.19 (dd, *J* = 8.0, 1.6 Hz, 1H), 7.58 – 7.42 (m, 6H), 6.91 – 6.81 (m, 1H), 6.11 (s, 1H), 5.59 (s, 3H), 5.14 (s, 2H), 5.05 (s, 1H), 4.24 (t, *J* = 5.3 Hz, 2H), 3.53 (q, *J* = 5.5 Hz, 2H), 1.93 (s, 2H).

<sup>13</sup>C NMR (101 MHz, Chloroform-*d*, δ, ppm): 167.26, 156.14, 147.46, 141.21, 136.05, 135.90, 134.17, 129.49, 129.43, 128.66, 127.53, 126.10, 125.78, 118.76, 65.89, 63.62, 45.82, 40.29, 18.29.

ESI-MS: *m/z* calc. for C<sub>21</sub>H<sub>22</sub>N<sub>4</sub>O<sub>7</sub>Na<sup>+</sup> 465.1381; Found: [M + Na]<sup>+</sup> = 465.1373.

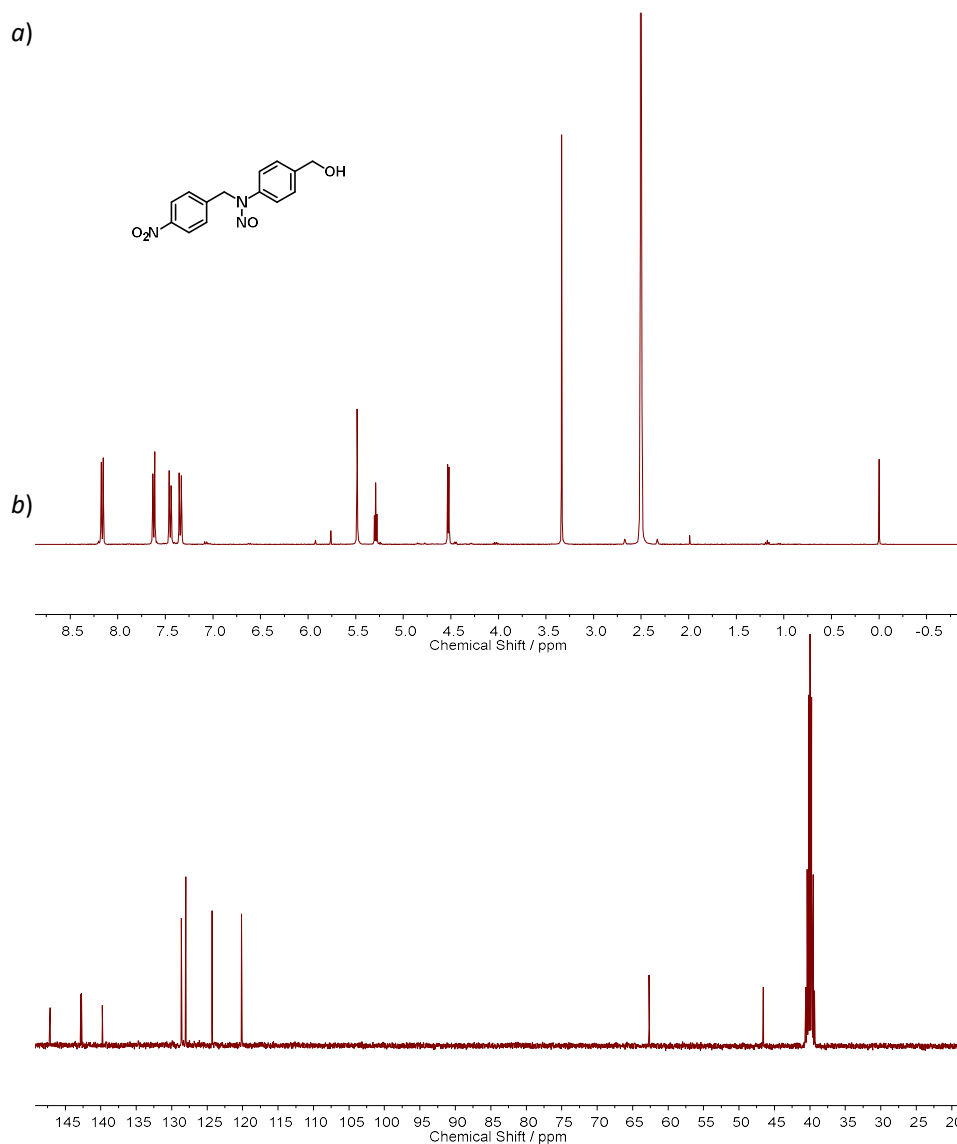


**Figure S3.** (a)  $^1\text{H}$  and (b)  $^{13}\text{C}$  NMR spectra recorded in  $\text{DMSO-}d_6$  for *N*-(4-(hydroxymethyl)phenyl)-*N*-(4-nitrobenzyl)nitrous amide.

$^1\text{H}$  NMR (400 MHz,  $\text{DMSO-}d_6$ ,  $\delta$ , ppm): 8.16 (d,  $J = 8.7$  Hz, 2H), 7.62 (d,  $J = 8.5$  Hz, 2H), 7.45 (d,  $J = 8.5$  Hz, 2H), 7.34 (d,  $J = 8.8$  Hz, 2H), 5.48 (s, 2H), 5.29 (t,  $J = 5.7$  Hz, 1H), 4.53 (d,  $J = 5.7$  Hz, 2H).

$^{13}\text{C}$  NMR (101 MHz,  $\text{DMSO-}d_6$ ,  $\delta$ , ppm): 147.17, 142.78, 139.80, 128.64, 128.02, 124.29, 120.13, 62.67, 46.59, 40.17.

ESI-MS:  $m/z$  calc. for  $\text{C}_{14}\text{H}_{13}\text{N}_3\text{O}_4\text{Na}^+$  310.0798; Found:  $[\text{M} + \text{Na}]^+ = 310.0804$ .

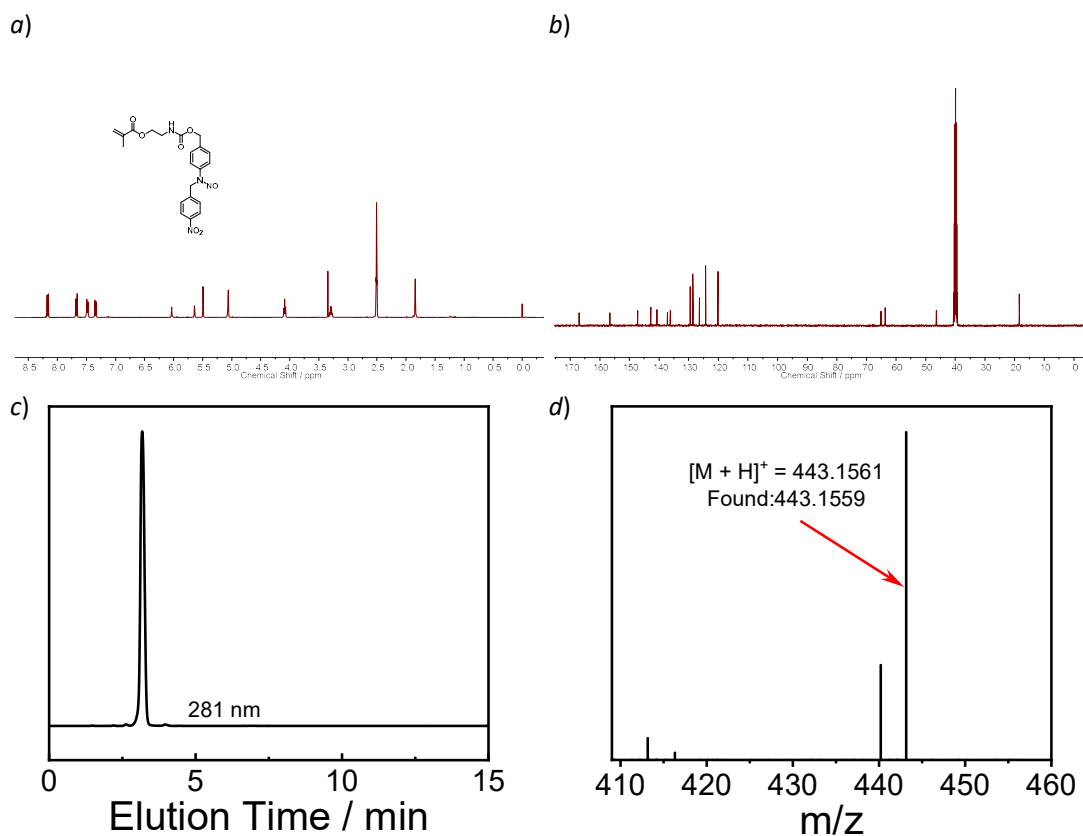


**Figure S4.** (a)  $^1\text{H}$  and (b)  $^{13}\text{C}$  NMR spectra recorded in  $\text{CDCl}_3$  for *p*NBN monomer. (c) HPLC profile recorded at 281 nm for *p*NBN monomer (1 mM;  $\text{CH}_3\text{CN}/\text{H}_2\text{O}$ , v/v = 7/3 (0-3 min), 7/3-9/1 (3-15 min) as the eluent). (d) ESI mass spectrum recorded for *p*NBN monomer.

$^1\text{H}$  NMR (400 MHz,  $\text{DMSO}-d_6$ ,  $\delta$ , ppm): 8.21 – 8.10 (d, 2H), 7.67 (d,  $J = 8.6$  Hz, 2H), 7.48 (d,  $J = 8.4$  Hz, 3H), 7.34 (d,  $J = 8.8$  Hz, 2H), 6.03 (s, 1H), 5.64 (s, 1H), 5.49 (s, 2H), 5.06 (s, 2H), 4.09 (t,  $J = 5.5$  Hz, 2H), 3.29 (q,  $J = 5.6$  Hz, 2H), 1.84 (s, 3H).

$^{13}\text{C}$  NMR (400 MHz,  $\text{DMSO}-d_6$ ,  $\delta$ , ppm): 166.96, 156.63, 147.18, 142.75, 140.67, 137.19, 136.20, 129.50, 128.59, 126.39, 124.31, 120.11, 65.05, 63.72, 46.35, 40.15, 18.40.

ESI-MS:  $m/z$  calc. for  $\text{C}_{21}\text{H}_{22}\text{N}_4\text{O}_7\text{H}^+$  443.1561; Found:  $[\text{M} + \text{H}]^+ = 443.1559$ .

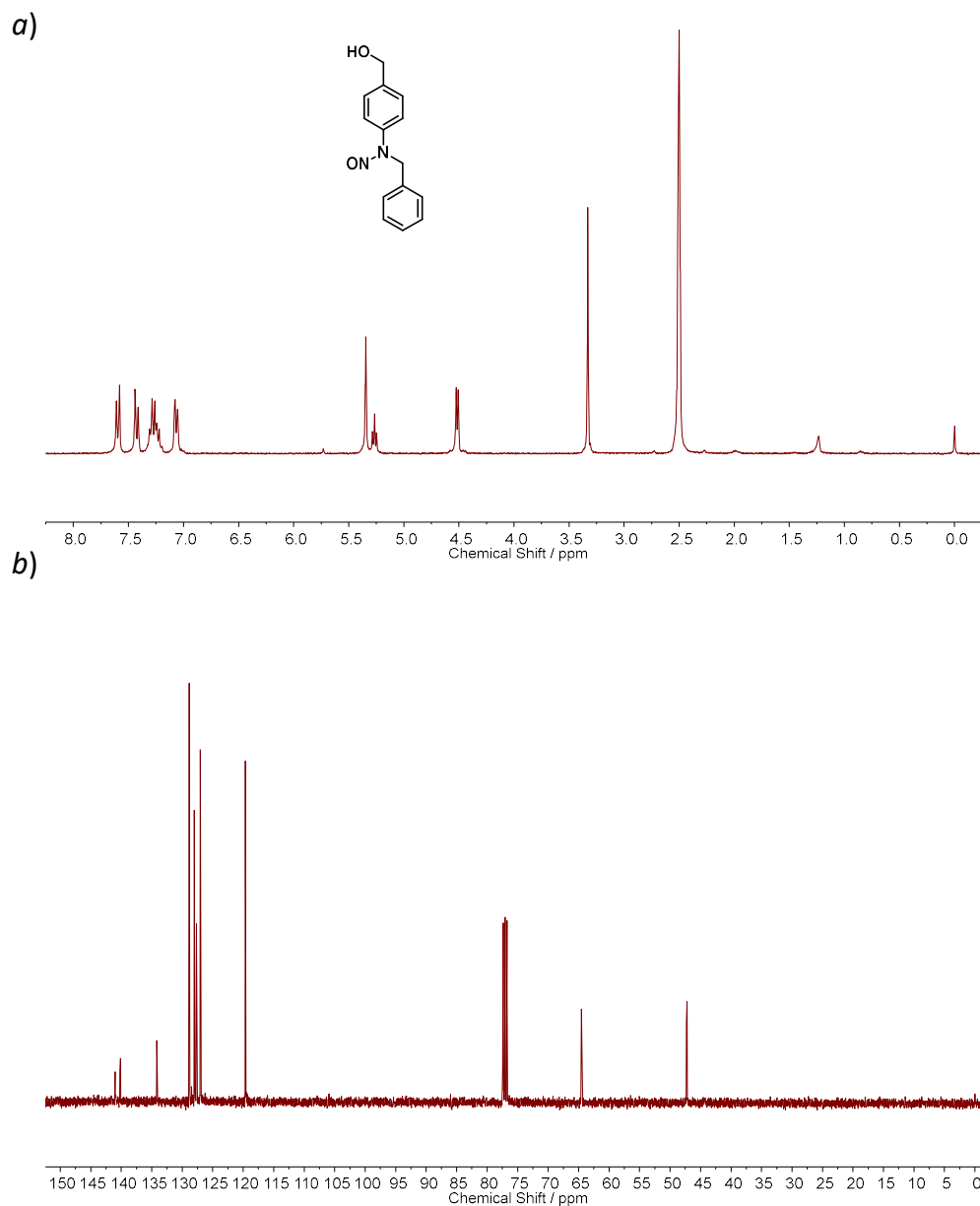


**Figure S5.** (a)  $^1\text{H}$  and (b)  $^{13}\text{C}$  NMR spectra for *N*-benzyl-*N*-(4-(hydroxymethyl) phenyl)nitrous amide.

$^1\text{H}$  NMR (400 MHz,  $\text{DMSO-}d_6$ ,  $\delta$ , ppm): 7.72 – 7.51 (m, 2H), 7.43 (d,  $J = 8.3$  Hz, 2H), 7.26 (dt,  $J = 12.2, 6.8$  Hz, 3H), 7.07 (d,  $J = 7.3$  Hz, 2H), 5.34 (s, 2H), 5.27 (t,  $J = 5.7$  Hz, 1H), 4.52 (d,  $J = 5.7$  Hz, 2H).

$^{13}\text{C}$  NMR (101 MHz,  $\text{Chloroform-}d$ ,  $\delta$ , ppm): 141.02, 140.11, 134.17, 128.85, 128.00, 127.66, 127.02, 119.64, 64.55, 47.23.

ESI-MS:  $m/z$  calc. for  $\text{C}_{14}\text{H}_{15}\text{N}_2\text{O}_2^+$  243.1128; Found:  $[\text{M} + \text{H}]^+ = 243.1133$ .

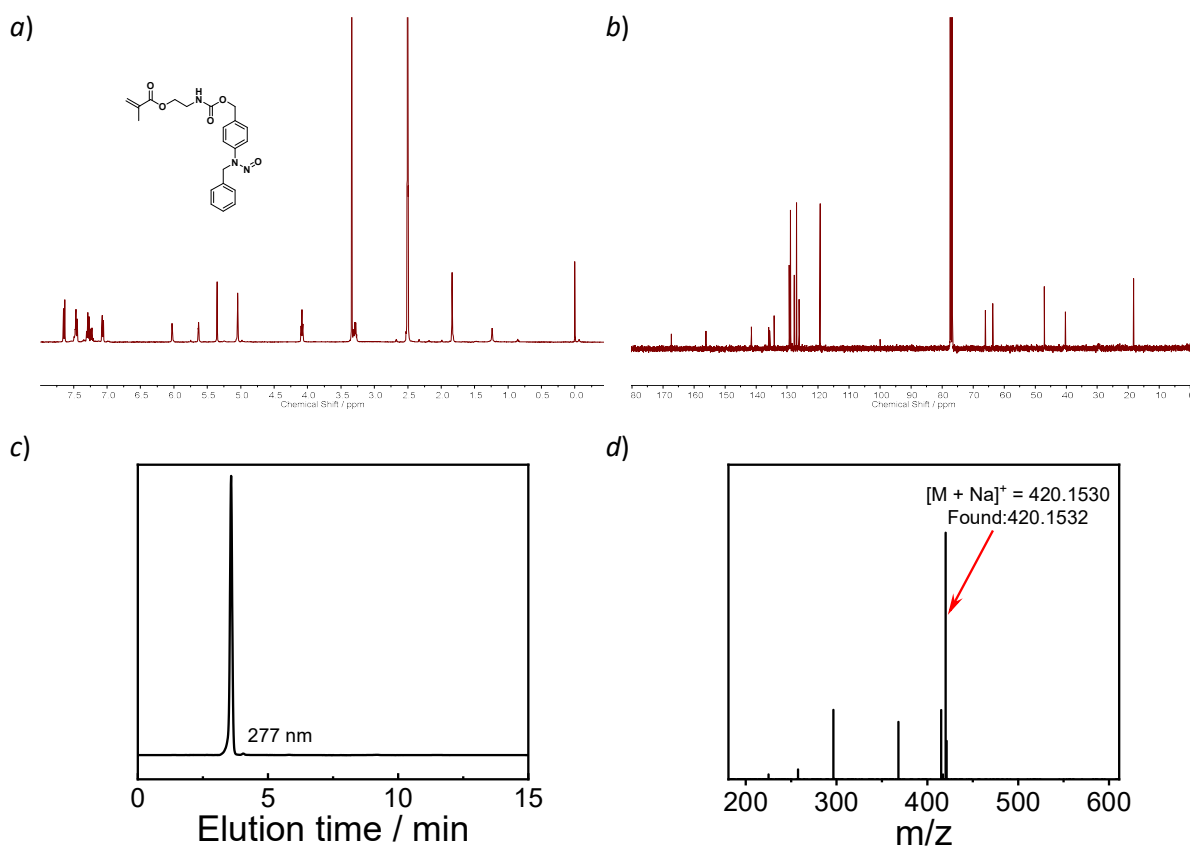


**Figure S6.** (a) <sup>1</sup>H and (b) <sup>13</sup>C NMR spectra recorded for BN monomer in (a) DMSO-*d*<sub>6</sub> and (b) CDCl<sub>3</sub>, respectively. (c) HPLC elution profile recorded at 277 nm for BN monomer (1 mM; CH<sub>3</sub>CN/H<sub>2</sub>O, v/v = 7/3 (0-3 min), 7/3-9/1 (3-15 min) as the eluent). (d) ESI mass spectrum recorded for BN monomer.

<sup>1</sup>H NMR (400 MHz, DMSO-*d*<sub>6</sub>, δ, ppm): 7.68 – 7.60 (m, 2H), 7.51 – 7.41 (m, 3H), 7.33 – 7.19 (m, 3H), 7.10 – 7.03 (m, 2H), 6.15 – 5.92 (m, 1H), 5.63 (t, *J* = 1.7 Hz, 1H), 5.35 (s, 2H), 5.04 (s, 2H), 4.08 (t, *J* = 5.5 Hz, 2H), 3.33 – 3.25 (m, 2H), 1.84 (s, 3H).

<sup>13</sup>C NMR (101 MHz, Chloroform-*d*, δ, ppm): 167.28, 156.14, 141.53, 135.90, 135.58, 134.14, 129.29, 128.87, 127.67, 126.92, 126.12, 119.35, 66.05, 63.65, 47.06, 40.31, 18.31.

ESI-MS: m/z calc. for C<sub>21</sub>H<sub>23</sub>N<sub>3</sub>O<sub>5</sub>Na<sup>+</sup> 420.1530; Found: [M + Na]<sup>+</sup> = 420.1532.

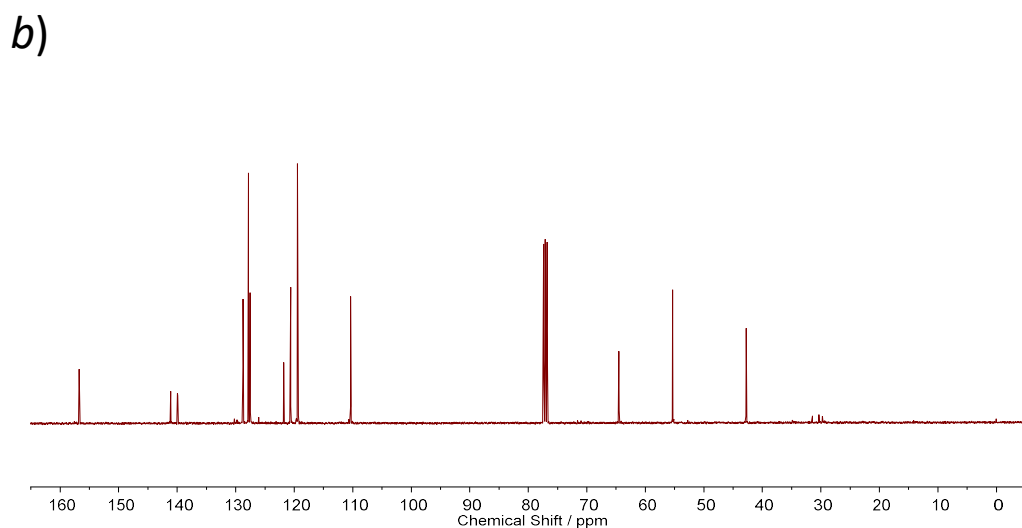
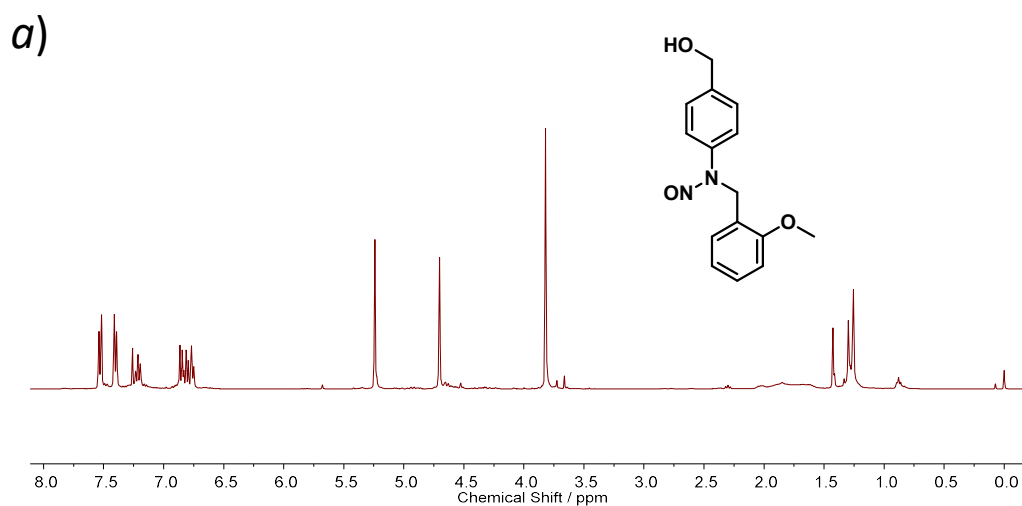


**Figure S7.** (a)  $^1\text{H}$  and (b)  $^{13}\text{C}$  NMR spectra for *N*-(4-(hydroxymethyl)phenyl)-*N*-(2-methoxybenzyl)nitrous amide.

$^1\text{H}$  NMR (400 MHz, Chloroform-*d*,  $\delta$ , ppm): 7.53 (d,  $J = 8.4$  Hz, 2H), 7.40 (d,  $J = 8.1$  Hz, 2H), 7.21 (t,  $J = 7.7$  Hz, 1H), 6.88 – 6.73 (m, 3H), 5.24 (s, 2H), 4.70 (s, 2H), 3.82 (s, 3H).

$^{13}\text{C}$  NMR (101 MHz, Chloroform-*d*,  $\delta$ , ppm): 156.73, 141.09, 139.93, 128.76, 127.84, 127.55, 121.79, 120.62, 119.42, 110.36, 64.53, 55.33, 42.78.

ESI-MS:  $m/z$  calc. for  $\text{C}_{15}\text{H}_{16}\text{N}_2\text{O}_3\text{Na}^+$  295.1053; Found:  $[\text{M} + \text{Na}]^+ = 295.1059$ .



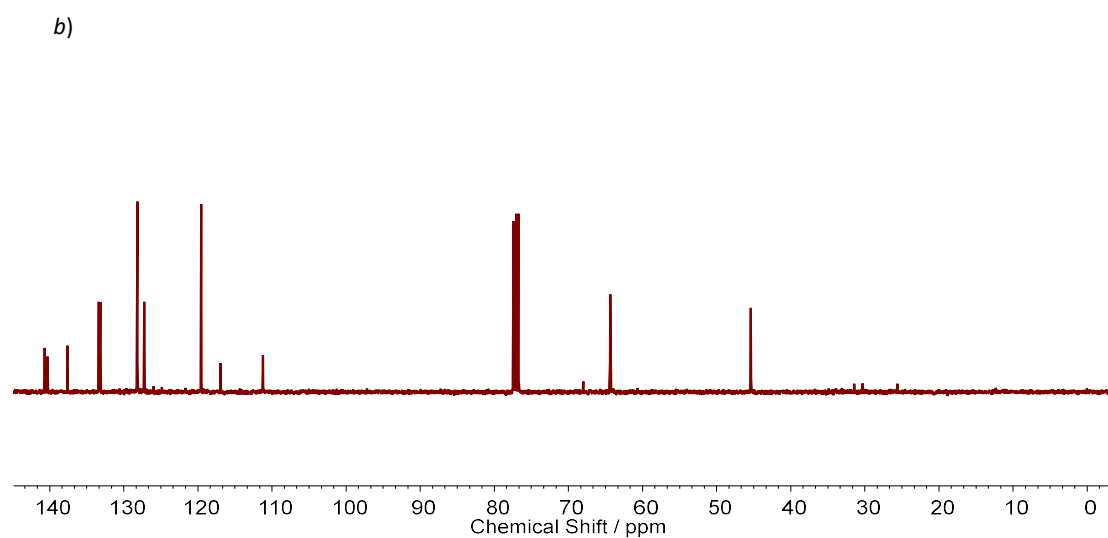
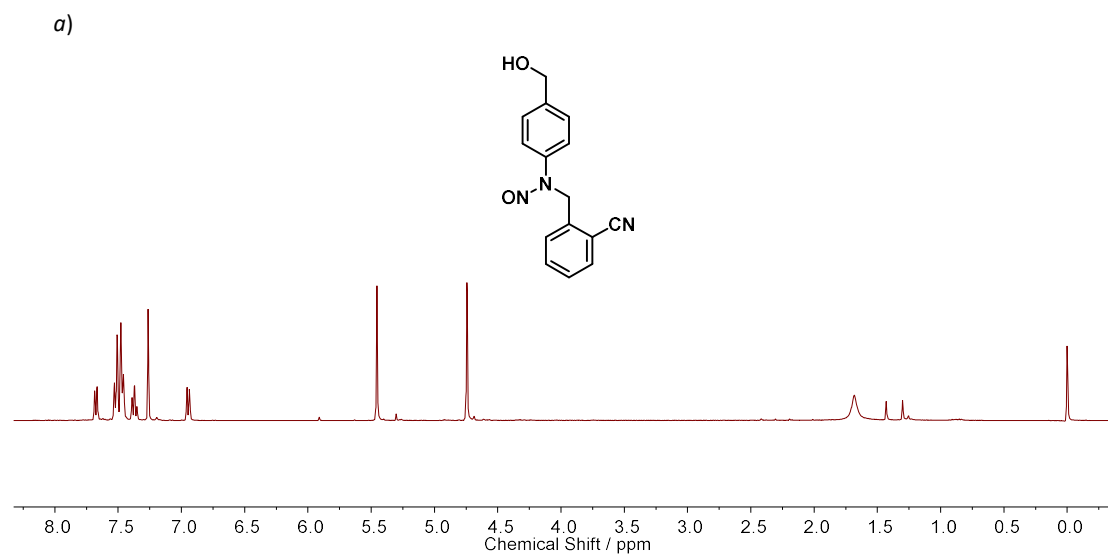


**Figure S8.** (a)  $^1\text{H}$  and (b)  $^{13}\text{C}$  NMR spectra for *N*-(2-cyanobenzyl)-*N*-(4-(hydroxymethyl)phenyl)nitrous amide.

$^1\text{H}$  NMR (400 MHz, Chloroform-*d*,  $\delta$ , ppm): 7.68 (d,  $J = 7.7$  Hz, 1H), 7.54 – 7.44 (m, 5H), 7.37 (t,  $J = 7.6$  Hz, 1H), 6.95 (d,  $J = 7.9$  Hz, 1H), 5.46 (s, 2H), 4.74 (s, 2H).

$^{13}\text{C}$  NMR (101 MHz, Chloroform-*d*,  $\delta$ , ppm): 140.68, 140.29, 137.59, 133.38, 133.15, 128.23, 128.17, 127.25, 119.56, 116.95, 111.23, 64.36, 45.37.

ESI-MS:  $m/z$  calc. for  $\text{C}_{15}\text{H}_{13}\text{N}_3\text{O}_2\text{Na}^+$  290.0900; Found:  $[\text{M} + \text{Na}]^+ = 290.0899$ .

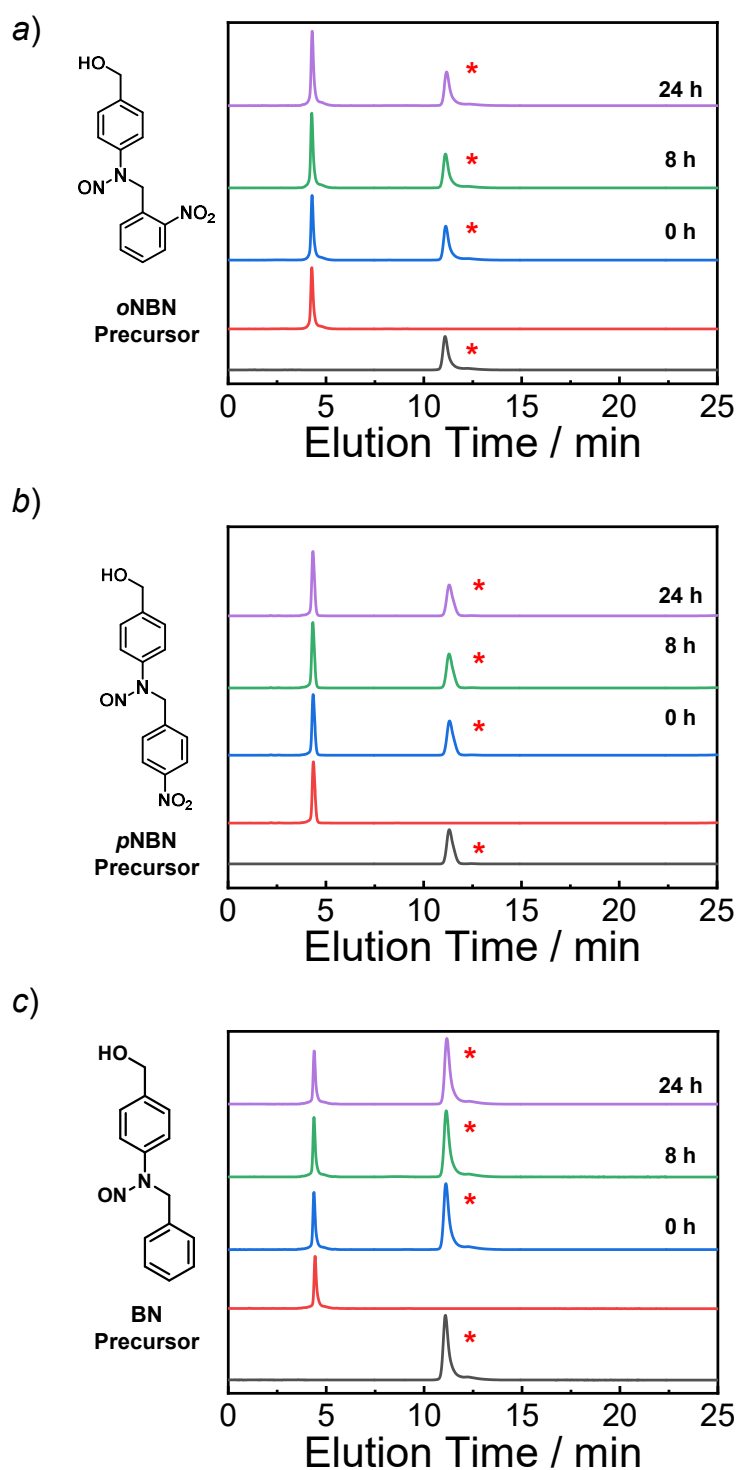


**Figure S9.** HPLC profiles recorded at 254 nm for (a) *o*NBN, (b) *p*NBN, and (c) BN precursors (0.5 mM; CH<sub>3</sub>CN/H<sub>2</sub>O, v/v = 1/1 as the eluent) upon heating at 70 °C in CH<sub>3</sub>CN for varying times (0, 8, and 24 h). The asterisks represent the elution peaks of coumarin 102 internal standard.

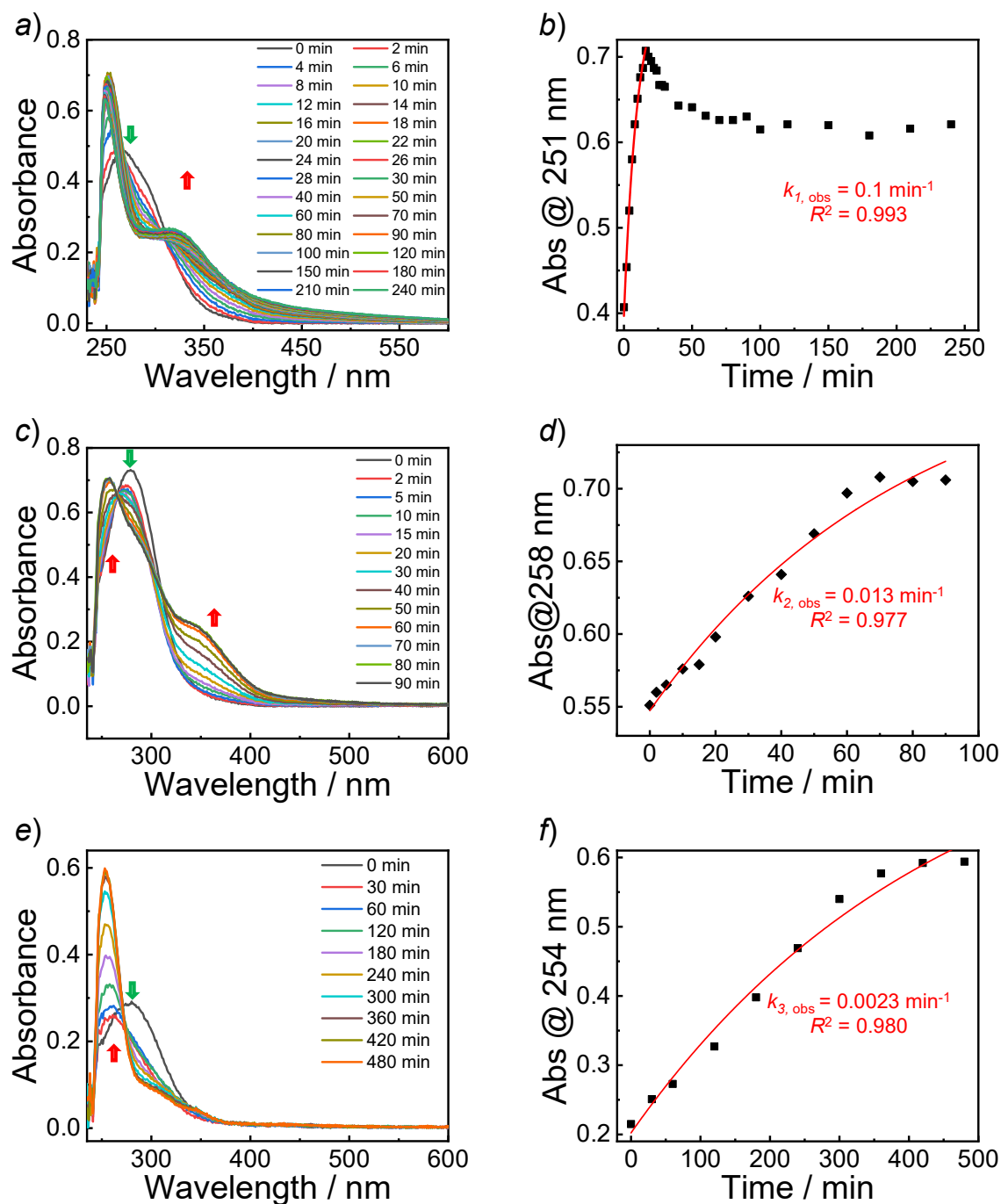


**Figure S10.** (a,c,e) Evolution of UV-vis spectroscopy and (b,d,f) absorbance intensity changes (solid squares) together with a mono-exponential fit of (a,b) *o*NBN, (c,d) *p*NBN, and (e,f) BN solutions (40  $\mu\text{M}$ ; 20 mM PBS buffer containing 40% DMSO; pH 7.4) under UV 365 nm irradiation (4  $\text{mW}/\text{cm}^2$ ).

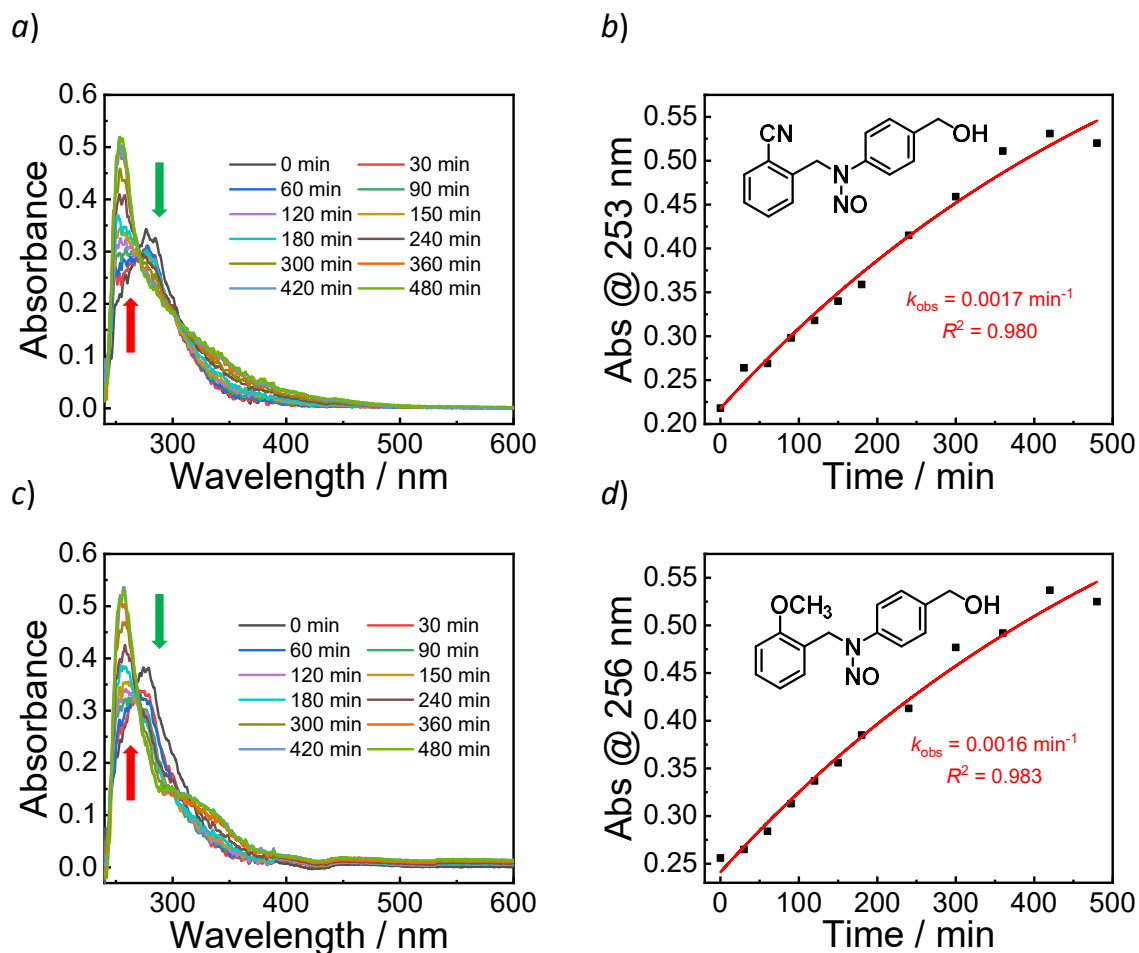


**Figure S11.** (a,c) Evolution of UV-vis spectroscopy and (b,d) absorbance intensity changes (solid squares) together with a mono-exponential fit of (a,b) *N*-(2-cyanobenzyl)-*N*-(4-(hydroxymethyl)phenyl)nitrous amide and (c,d) *N*-(4-(hydroxymethyl)phenyl)-*N*-(2-methoxybenzyl)nitrous amide (40  $\mu\text{M}$ ; 20 mM PBS buffer containing 40% DMSO; pH 7.4) under UV 365 nm irradiation (4  $\text{mW}/\text{cm}^2$ ).

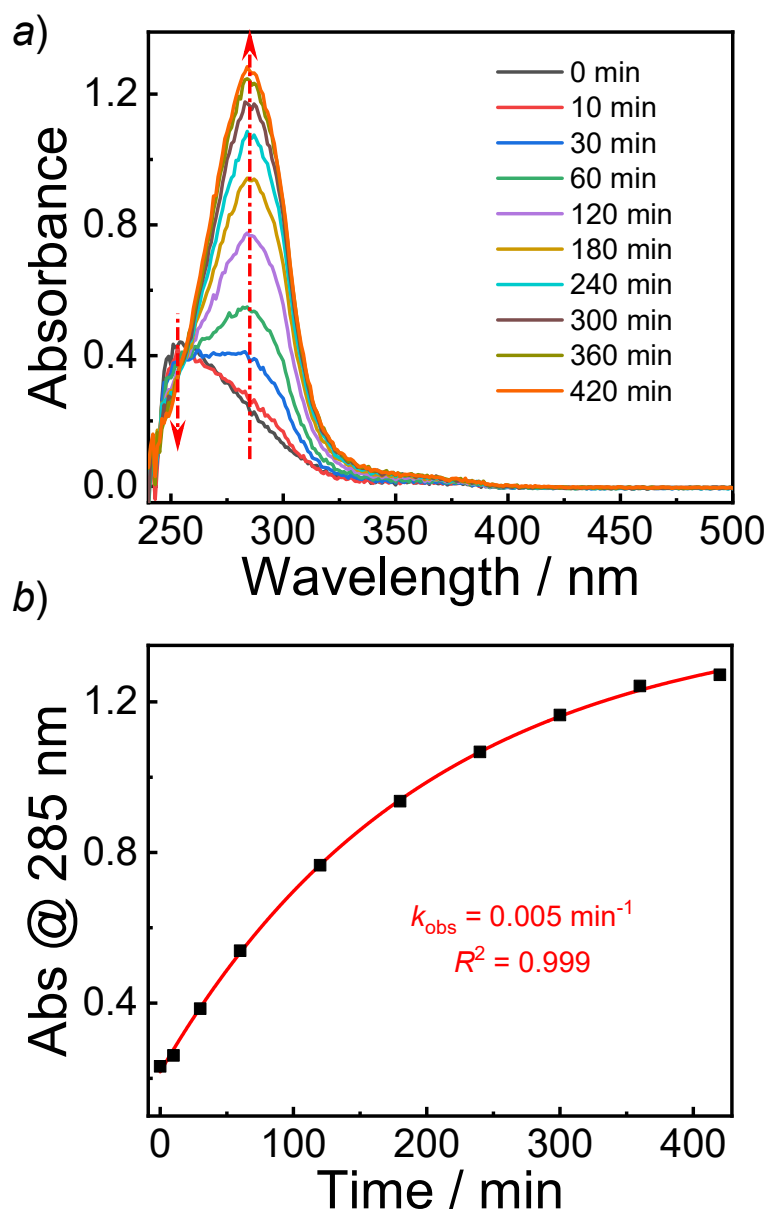


**Figure S12.** (a) Absorbance spectra and (b) absorbance intensity changes (solid squares) together with a mono-exponential fit (red line) of aqueous solution (20 mM PBS buffer, pH 7.4; 40% DMSO) of **BNN6** (40  $\mu\text{M}$ ) under UV light irradiation (4  $\text{mW}/\text{cm}^2$ ).

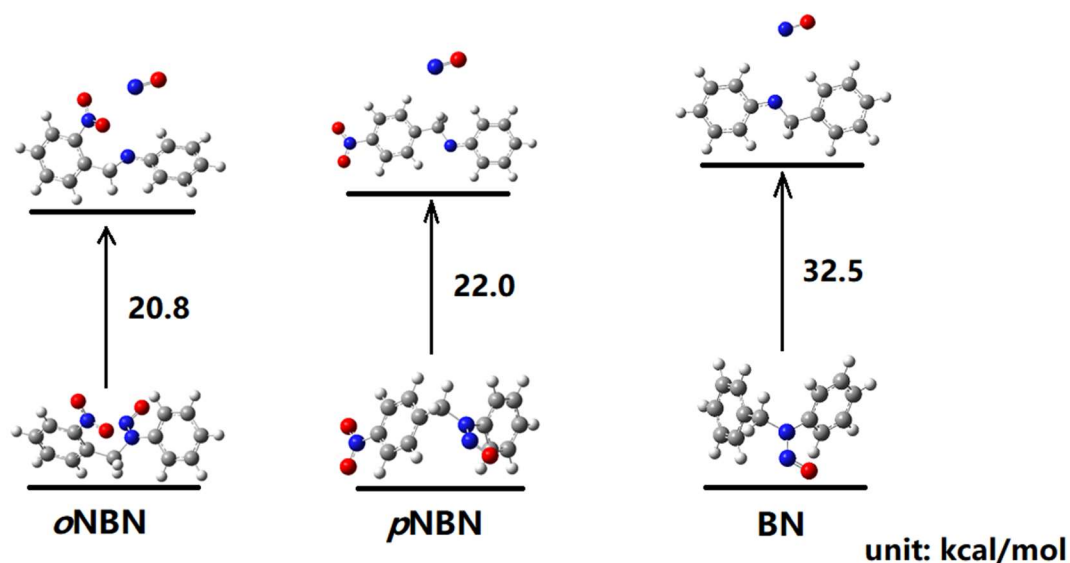


**Figure S13.** Calculation of the bond dissociation energy (BDE) of the *o*NBN, *p*NBN, and BN monomers. To rationale the difference of NO release rates in *o*NBN, *p*NBN and BN, we computed the N-N bond dissociation energies of their corresponding simplified model molecules using Gaussian 09<sup>1</sup> program. The geometries of related species were optimized at B3LYP<sup>2</sup>/6-31G(d)<sup>3</sup> level in gas phase and verified as true minima by harmonic vibrational frequency calculations at the same level of theory. Then single point energy calculations were performed at M06-2X<sup>4</sup>/6-311 + G(3df,2pd)<sup>5</sup> based on optimized structures. The N-N bond dissociation energy (BDE) is defined as the free energy change owing to the N-N bond dissociation,  $BDE = \Delta G_{(x\text{BN minus NO})} - (\Delta G_{(\text{NO})} + \Delta G_{(x\text{BN})})$ .

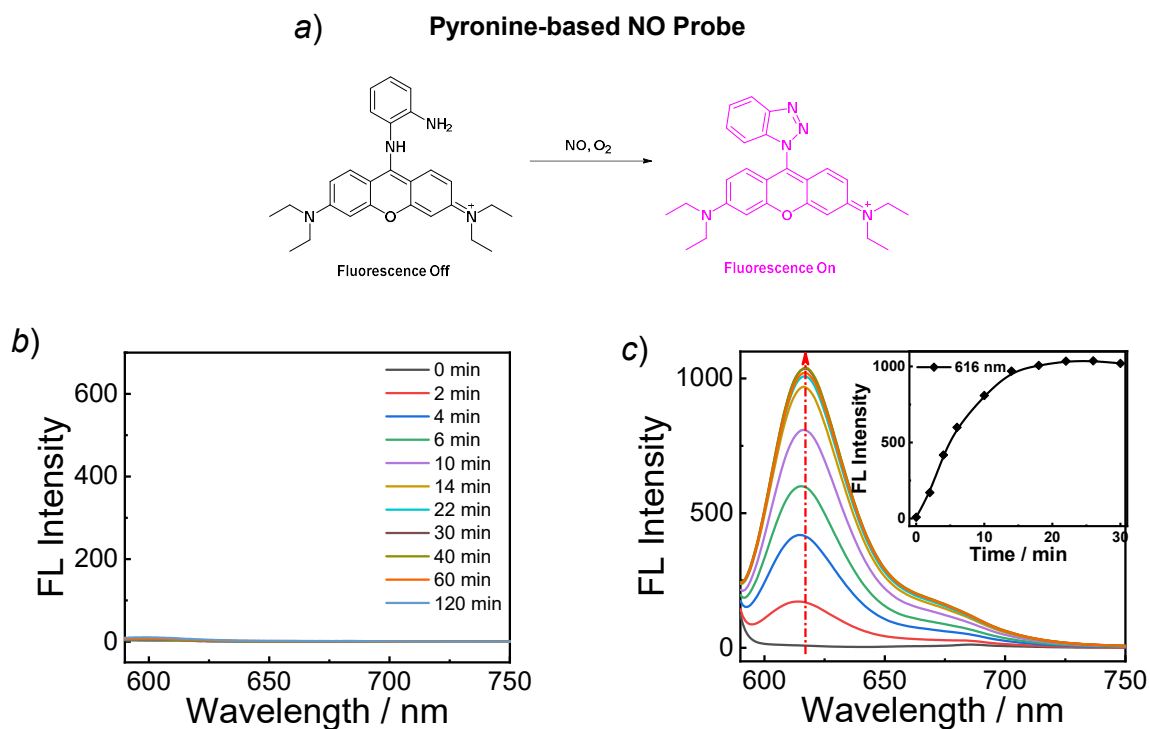


**Figure S14.** (a) Sensing Mechanism of pyronine-based NO probe. (b) Fluorescence emission spectra ( $\lambda_{\text{ex}} = 570 \text{ nm}$ ; slit widths: Ex. = 5.0 nm, Em. = 10.0 nm) of pyronin probe (0.1 mM; DMSO/H<sub>2</sub>O = 1/99, v/v) under UV 365 nm irradiation (4 mW/cm<sup>2</sup>). (c) Evolution of fluorescence spectra ( $\lambda_{\text{ex}} = 570 \text{ nm}$ ; slit widths: Ex. = 5.0 nm, Em. = 10.0 nm) recorded for the *o*NBN solution (40  $\mu\text{M}$ ; DMSO/H<sub>2</sub>O = 5/95, v/v) in the presence of pyronine probe (0.1 mM) under UV 365 nm irradiation (4 mW/cm<sup>2</sup>).

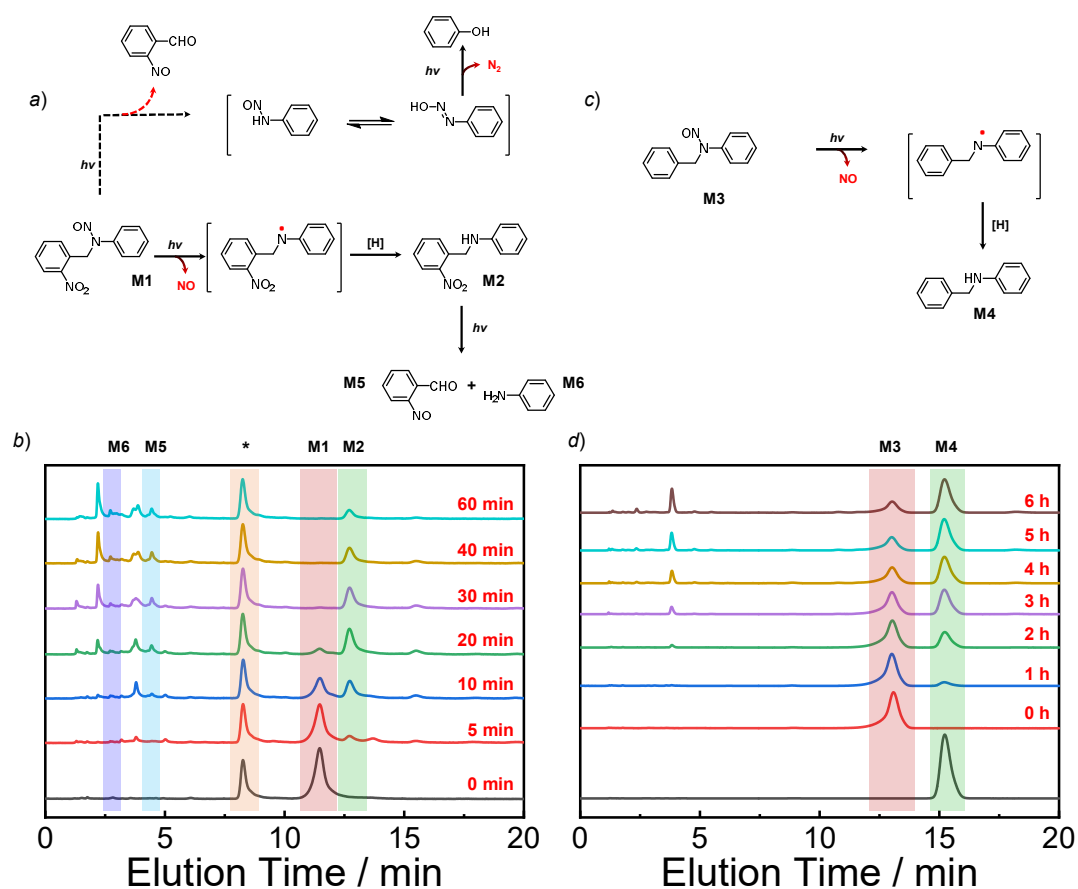


**Figure S15.** (a,c) Proposed degradation mechanism of *N*-(2-nitrobenzyl)-*N*-phenylnitrous amide (M1) and *N*-benzyl-*N*-phenylnitrous amide (M3) under light irradiation. (b,d) HPLC profiles detecting at 254 nm for (b) M1 and (d) M3 (0.25 mM; CH<sub>3</sub>CN/H<sub>2</sub>O, v/v = 1/1 as the eluent) under UV 365 nm irradiation (4 mW/cm<sup>2</sup>) for varying durations. The asterisk in (b) represents the signal of 4-bromo-1,8-naphthalic anhydride which was used as the internal standard.

**M1:** <sup>1</sup>H NMR (400 MHz, Chloroform-*d*,  $\delta$ , ppm): 8.19 (dt,  $J = 8.1, 1.0$  Hz, 1H), 7.59 – 7.51 (m, 3H), 7.52 – 7.43 (m, 3H), 7.42 – 7.34 (m, 1H), 6.89 (dd,  $J = 7.8, 1.4$  Hz, 1H), 5.60 (s, 2H).

<sup>13</sup>C NMR (101 MHz, Chloroform-*d*,  $\delta$ , ppm) 147.49, 141.55, 134.17, 129.76, 129.66, 128.62, 127.67, 127.63, 125.77, 118.90, 46.10.

ESI-MS:  $m/z$  calc. for C<sub>13</sub>H<sub>12</sub>N<sub>3</sub>O<sub>3</sub><sup>+</sup> 258.0873; Found: [M + H]<sup>+</sup> = 258.0869.

**M3:** <sup>1</sup>H NMR (400 MHz, Chloroform-*d*,  $\delta$ , ppm): 7.61 – 7.48 (m, 2H), 7.49 – 7.38 (m, 2H), 7.38 – 7.16 (m, 4H), 7.15 – 7.05 (m, 2H), 5.26 (s, 2H).



$^{13}\text{C}$  NMR (101 MHz, Chloroform-*d*,  $\delta$ , ppm): 141.79, 134.30, 129.51, 128.86, 127.63, 127.39, 127.01, 119.56, 47.36.

ESI-MS:  $m/z$  calc. for  $\text{C}_{13}\text{H}_{13}\text{N}_2\text{O}^+$  213.1022; Found:  $[\text{M} + \text{H}]^+ = 213.1019$ .

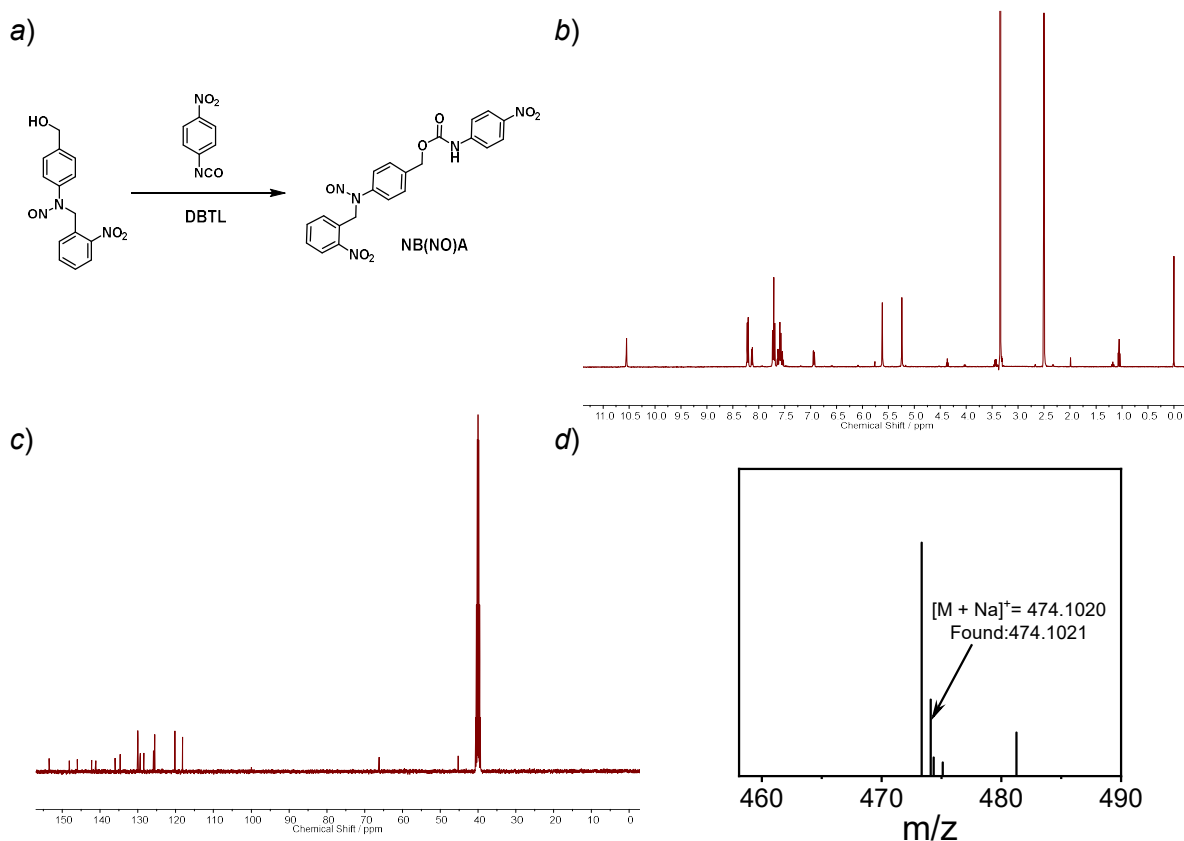


**Figure S16.** (a) Synthetic route employed for the preparation of NB(NO)A. (b) <sup>1</sup>H and (c) <sup>13</sup>C NMR spectra recorded in DMSO-*d*<sub>6</sub> for NB(NO)A. (d) ESI mass spectrum recorded for NB(NO)A.

<sup>1</sup>H NMR (400 MHz, DMSO-*d*<sub>6</sub>, δ, ppm): 10.55 (s, 1H), 8.21 (d, J = 9.3 Hz, 2H), 8.13 (dd, J = 8.1, 1.4 Hz, 1H), 7.78 – 7.66 (m, 4H), 7.66 – 7.51 (m, 4H), 6.94 (dd, J = 7.8, 1.4 Hz, 1H), 5.62 (s, 2H), 5.24 (s, 2H).

<sup>13</sup>C NMR (101 MHz, DMSO-*d*<sub>6</sub>, δ, ppm): 153.49, 148.10, 146.00, 142.22, 141.11, 136.03, 134.65, 130.02, 129.47, 129.35, 128.43, 125.86, 125.57, 120.19, 118.16, 66.20, 45.26.

ESI-MS: m/z calc. for C<sub>21</sub>H<sub>17</sub>N<sub>5</sub>O<sub>7</sub>Na<sup>+</sup> 474.1020; Found: [M + Na]<sup>+</sup> = 474.1021.

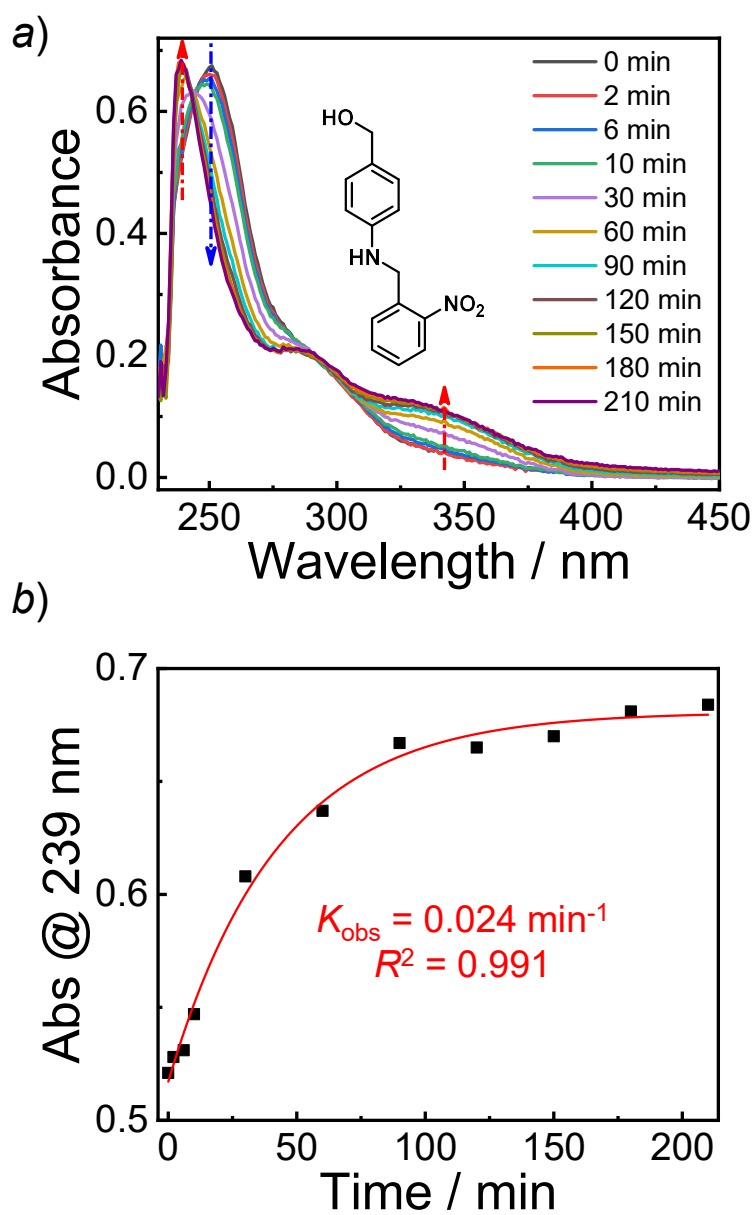


**Figure S17.** (a) Absorbance spectra, (b) absorbance intensity changes at 239 nm (blank squares) together with a mono-exponential fit of aqueous solution (20 mM PBS buffer, pH 7.4) of (4-((2-nitrobenzyl)amino)phenyl)methanol (40  $\mu\text{M}$ ) under UV 365 nm irradiation (4  $\text{mW}/\text{cm}^2$ ).

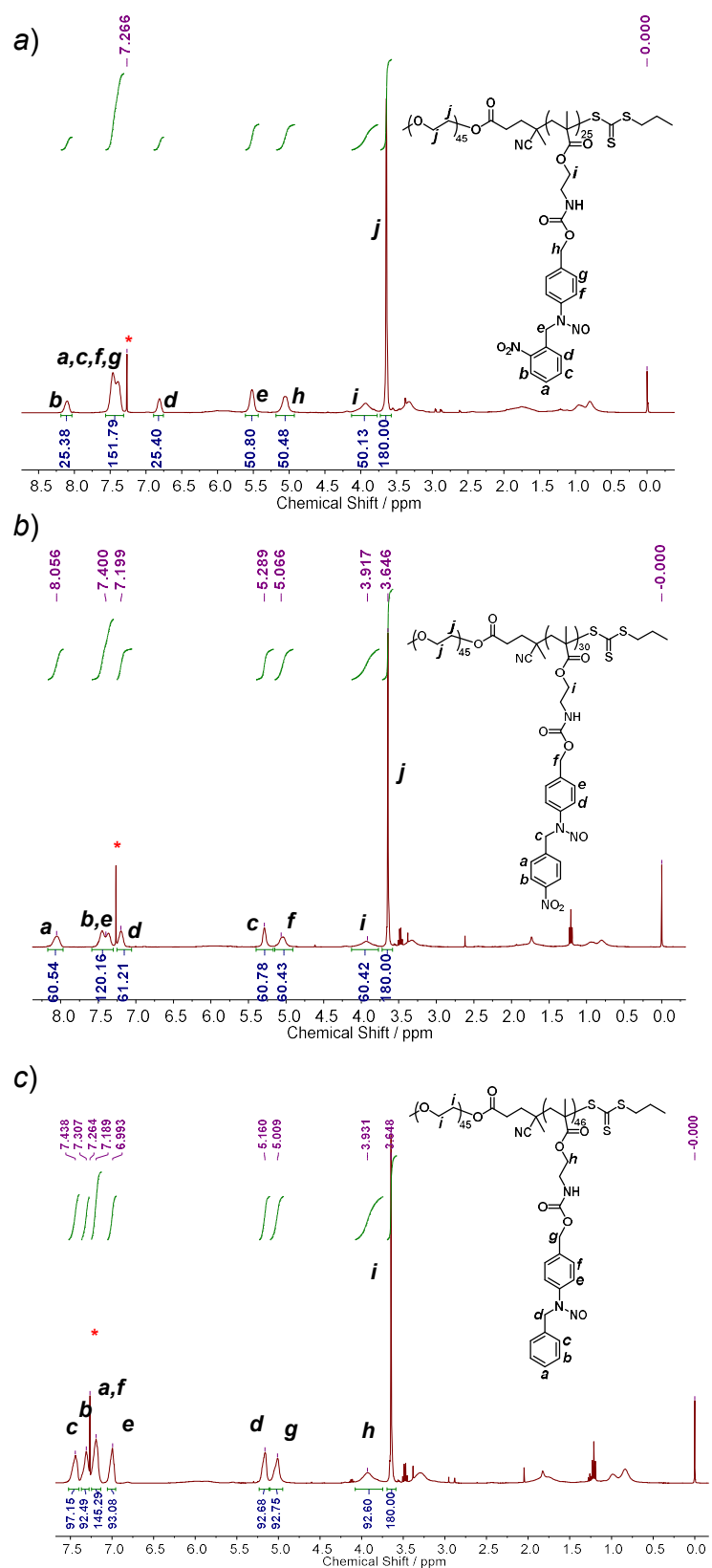


**Figure S18.**  $^1\text{H}$  NMR spectra recorded in  $\text{CDCl}_3$  for (a) BP1, (b) BP2, and (b) BP3 block copolymers. The asterisks denote the solvent signals.

**Table S1. Structural Parameters of the NO-Releasing Amphiphiles Used in This Study.**

Entry	Samples <sup>a</sup>	$M_{n,NMR}$ <sup>a</sup> (kDa)	$M_{n,GPC}$ <sup>b</sup> (kDa)	$M_w/M_n$ <sup>b</sup>	$\langle D_h \rangle /$ nm <sup>c</sup>	$\mu_2/\Gamma^2$ <sup>c</sup>	Nanostructure Morphology <sup>d</sup>	NO Payloads <sup>e</sup> ( $\mu\text{mol}/\text{mg}$ )
<b>BP1</b>	PEO <sub>45</sub> - <i>b</i> - P <sub>o</sub> NBN <sub>25</sub>	13.3	9	1.16	168	0.059	Vesicles	1.88
<b>BP2</b>	PEO <sub>45</sub> - <i>b</i> - P <sub>p</sub> NBN <sub>30</sub>	15.5	9.6	1.13	159	0.084	Vesicles	1.94
<b>BP3</b>	PEO <sub>45</sub> - <i>b</i> - PBN <sub>46</sub>	20.5	10.5	1.14	90	0.169	Micelles	2.24

<sup>a</sup> calculated from <sup>1</sup>H NMR results; <sup>b</sup> determined by GPC using THF as the eluent; <sup>c</sup> hydrodynamic diameter,  $\langle D_h \rangle$ , and polydispersity index,  $\mu_2/\Gamma^2$ , of nanoassemblies determined by DLS; <sup>d</sup> observed by transmission electron microscopy. <sup>e</sup> calculated from the <sup>1</sup>H NMR results.

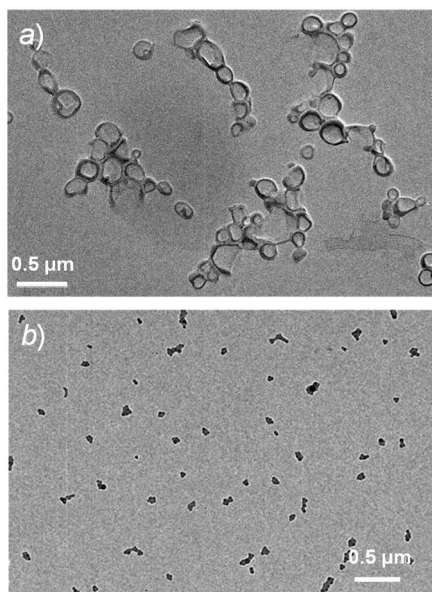


**Figure S19.** TEM images recorded for the aqueous dispersions (0.1 g/L) of (a) **BP2** vesicles and (b) **BP3** micellar nanoparticles.

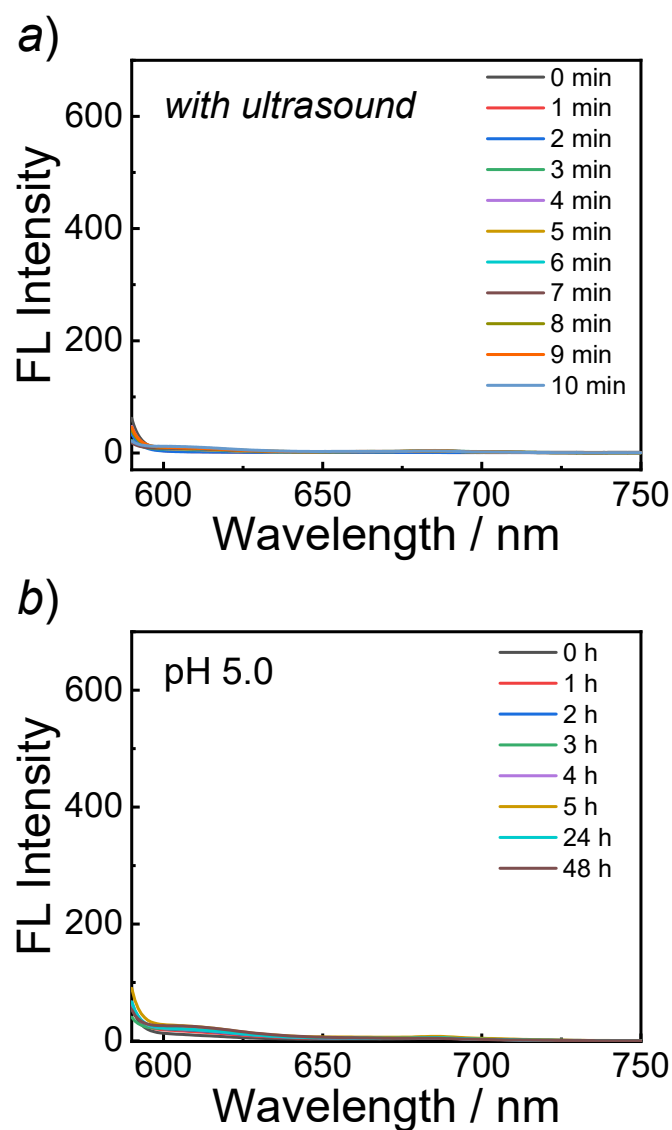


**Figure S20.** Fluorescence emission spectra ( $\lambda_{\text{ex}} = 570$  nm; slit widths: Ex. = 5.0 nm, Em. = 10.0 nm) of aqueous dispersion (0.2 g/L; [pyronin probe] = 0.1 mM; DMSO/H<sub>2</sub>O = 1/99, v/v) of **BP1** vesicles (a) under sonication and (b) at pH 5.0.

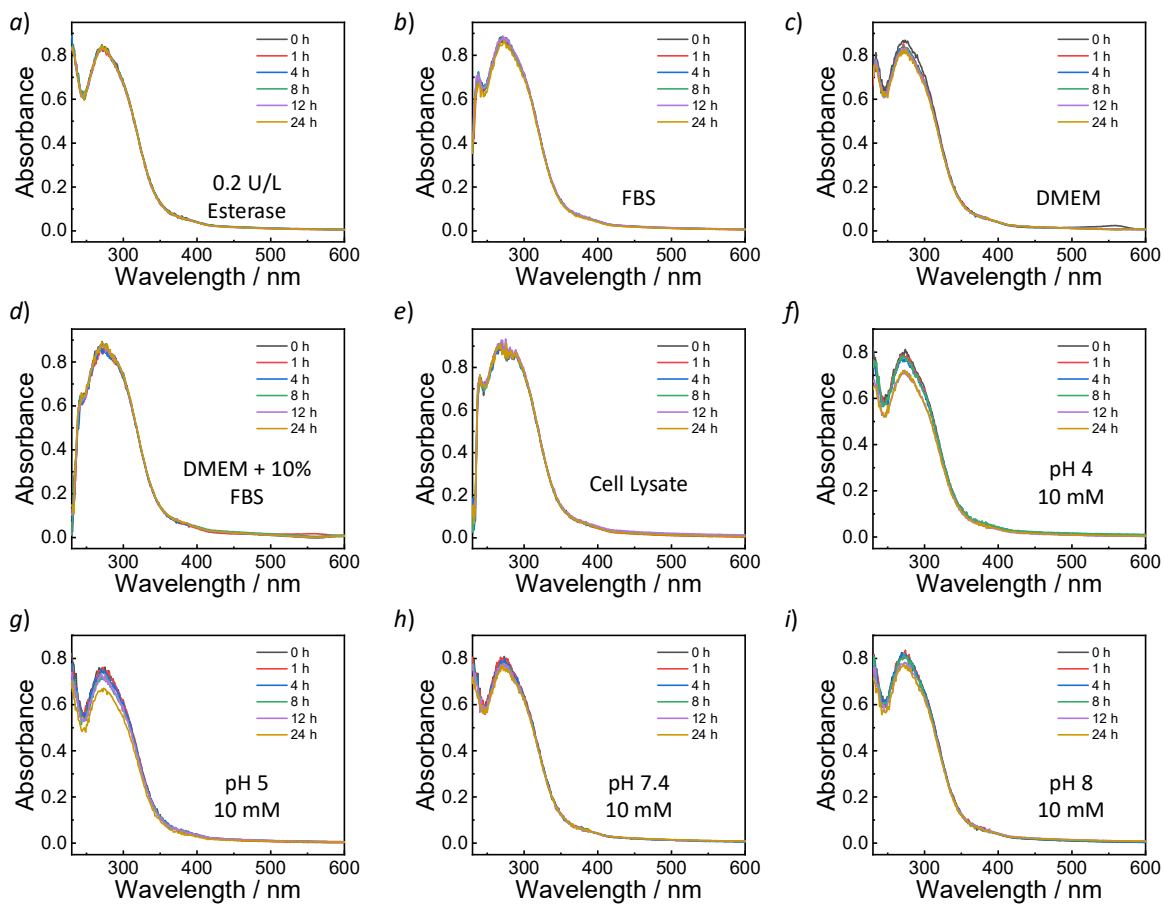


**Figure S21.** UV-vis absorbance of **BP1** vesicles (0.4 g/L) upon incubation with (a) 0.2 U/L esterase, (b) pure FBS, (c) pure DMEM, (d) DMEM with 10% FBS, (e) cell lysate (5,000,000 cells/mL), (f-i) buffer solutions with varying pH values.



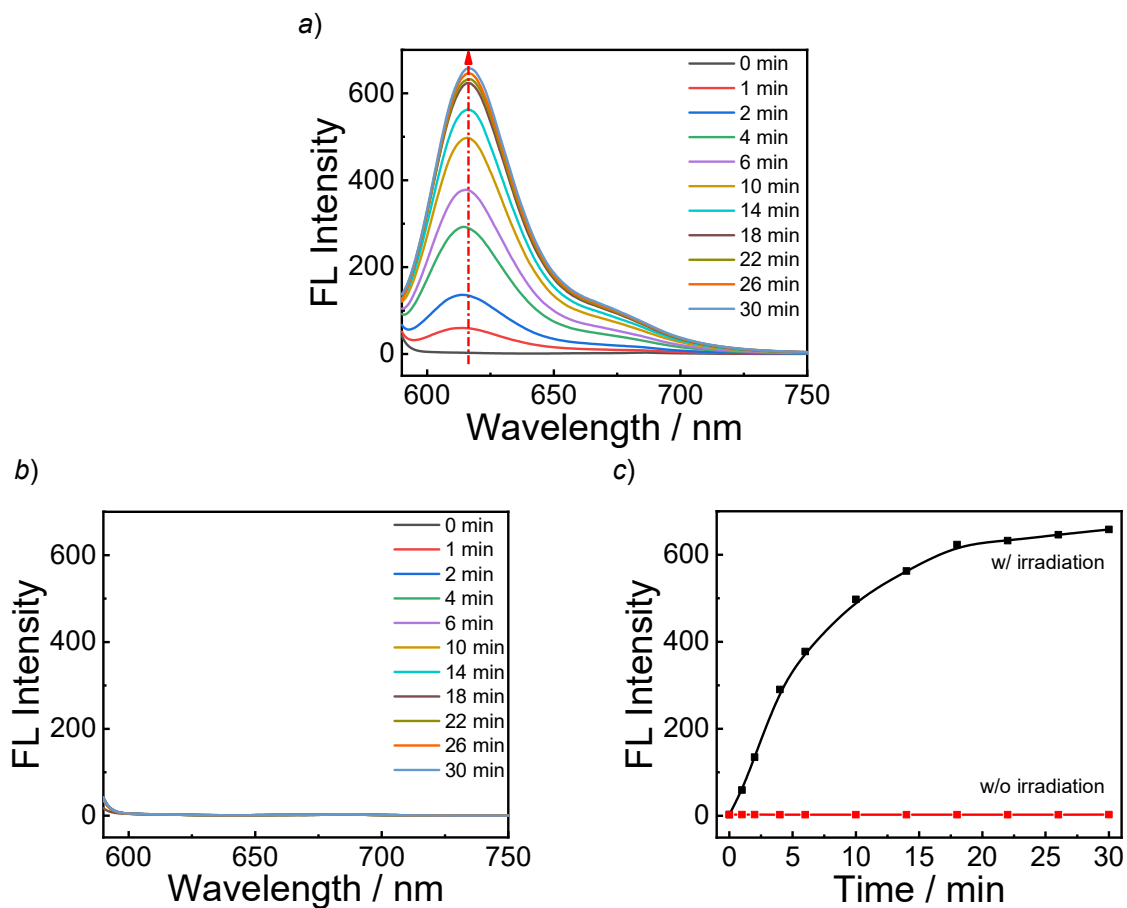


**Figure S22.** (a,b) Fluorescence emission spectra ( $\lambda_{\text{ex}} = 570 \text{ nm}$ ; slit widths: Ex. = 5.0 nm, Em. = 10.0 nm) and (c) fluorescence intensities changes at 616 nm of aqueous dispersions of **BP1** vesicles (0.1 g/L; [pyronin probe] = 0.1 mM; DMSO/H<sub>2</sub>O = 1/99, v/v) (a) under UV 365 nm irradiation and (b) without light irradiation.

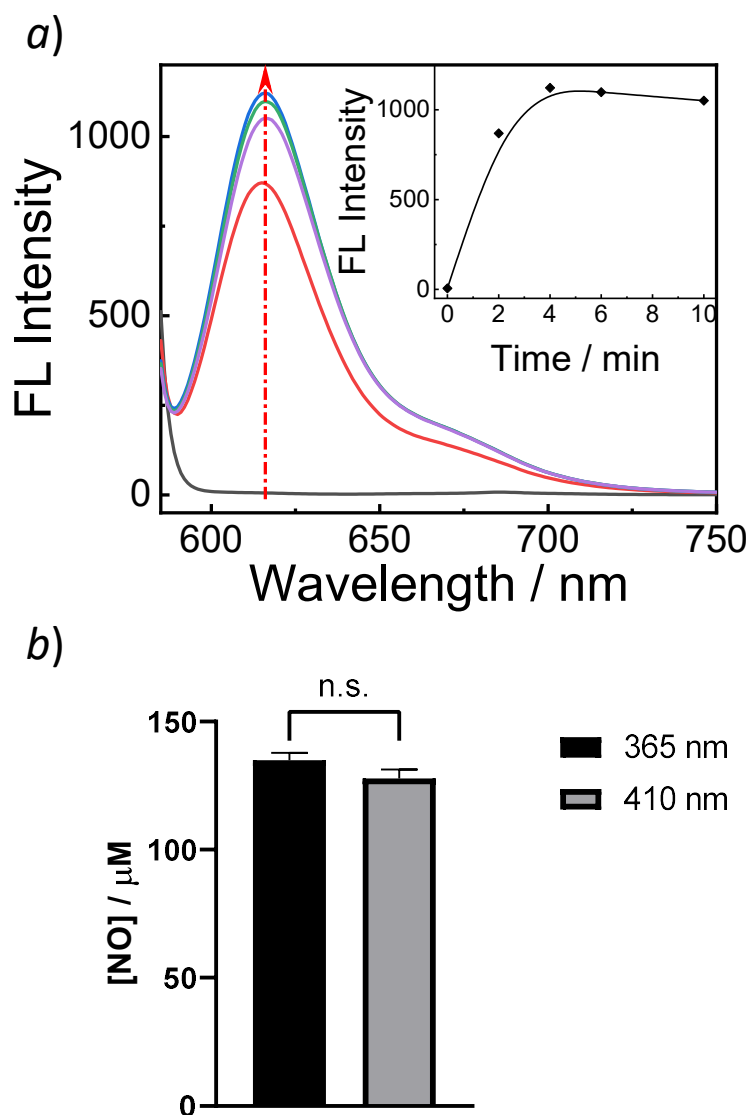


**Figure S23.** (a) Fluorescence emission spectra ( $\lambda_{\text{ex}} = 570 \text{ nm}$ ; slit widths: Ex. = 5.0 nm, Em. = 10.0 nm) of **BP1** vesicles (0.1 g/L; [pyronin probe] = 0.1 mM; DMSO/H<sub>2</sub>O = 1/99, v/v) under 410 nm visible light irradiation (30 mW/cm<sup>2</sup>). The inset shows the fluorescence intensity changes at 616 nm as a function of irradiation time. (b) Determination of the NO concentrations by Griess assay for **BP1** vesicles (0.1 g/L) after irradiation with 365 nm (4 mW/cm<sup>2</sup>) or 410 nm (30 mW/cm<sup>2</sup>) for 30 min (n.s.: not significant).

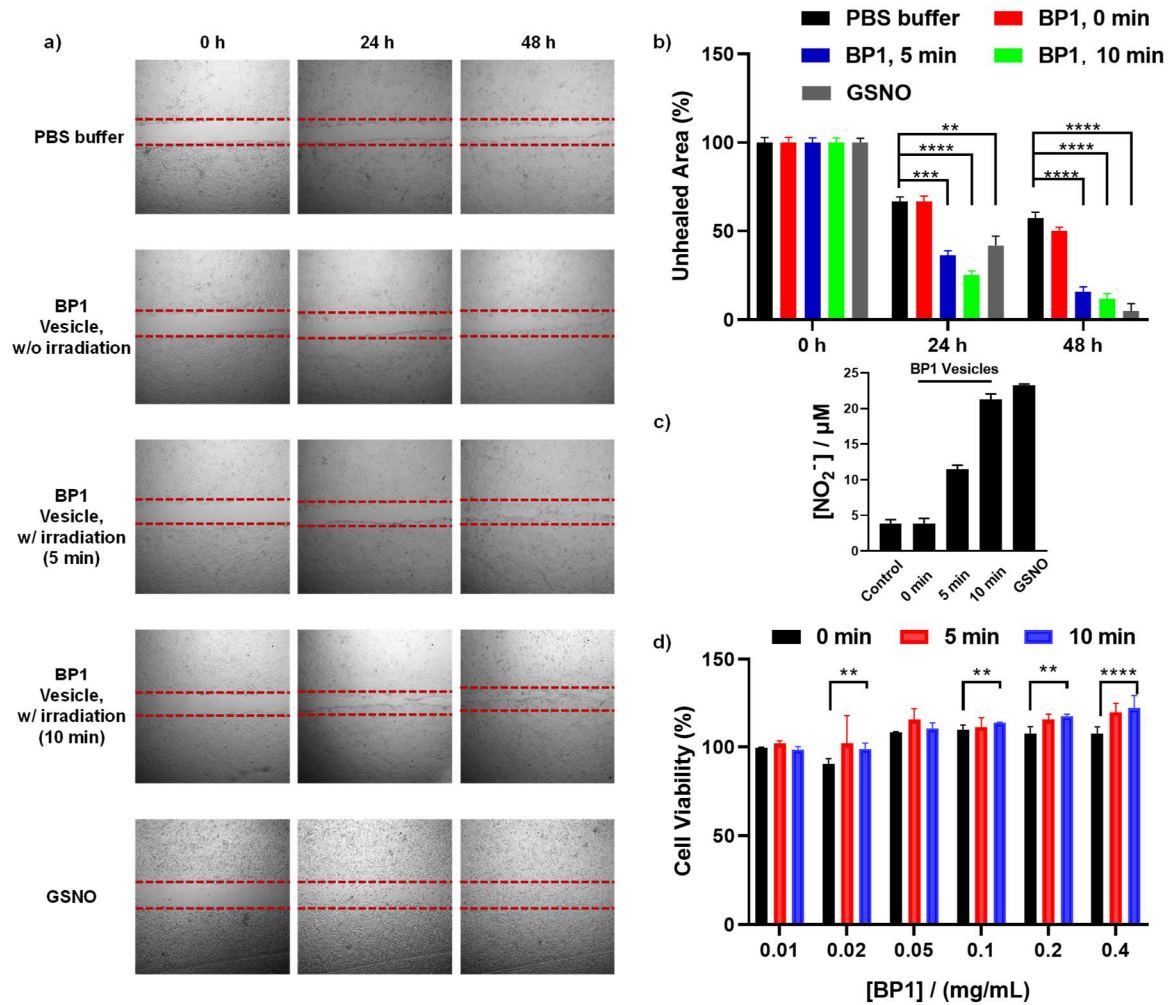


**Figure S24.** (a) Time-dependent photographs of *in vitro* scratch assay of human corneal epithelial cells (HCEC) under the treatment of PBS buffer and **BP1** vesicle dispersions with or without light irradiation. (b) Quantitative analysis of the unhealed scratch areas in (a) as calculated by ImageJ software. (c) Determination of the nitrite concentrations by Griess assay in the supernatant of cell culture medium with **BP1** vesicles (0.1 g/L) after irradiation with 0, 5, 10 min or in the presence of GSNO; the control sample was HCECs without any treatment; (d) Cytotoxicity assay of HCECs against **BP1** vesicles with or without light irradiation. Data are presented as mean  $\pm$  s.d. (n = 5); *p* values were calculated in comparison with the negative control. \*\* *p* < 0.01; \*\*\* *p* < 0.001; \*\*\*\* *p* < 0.0001.

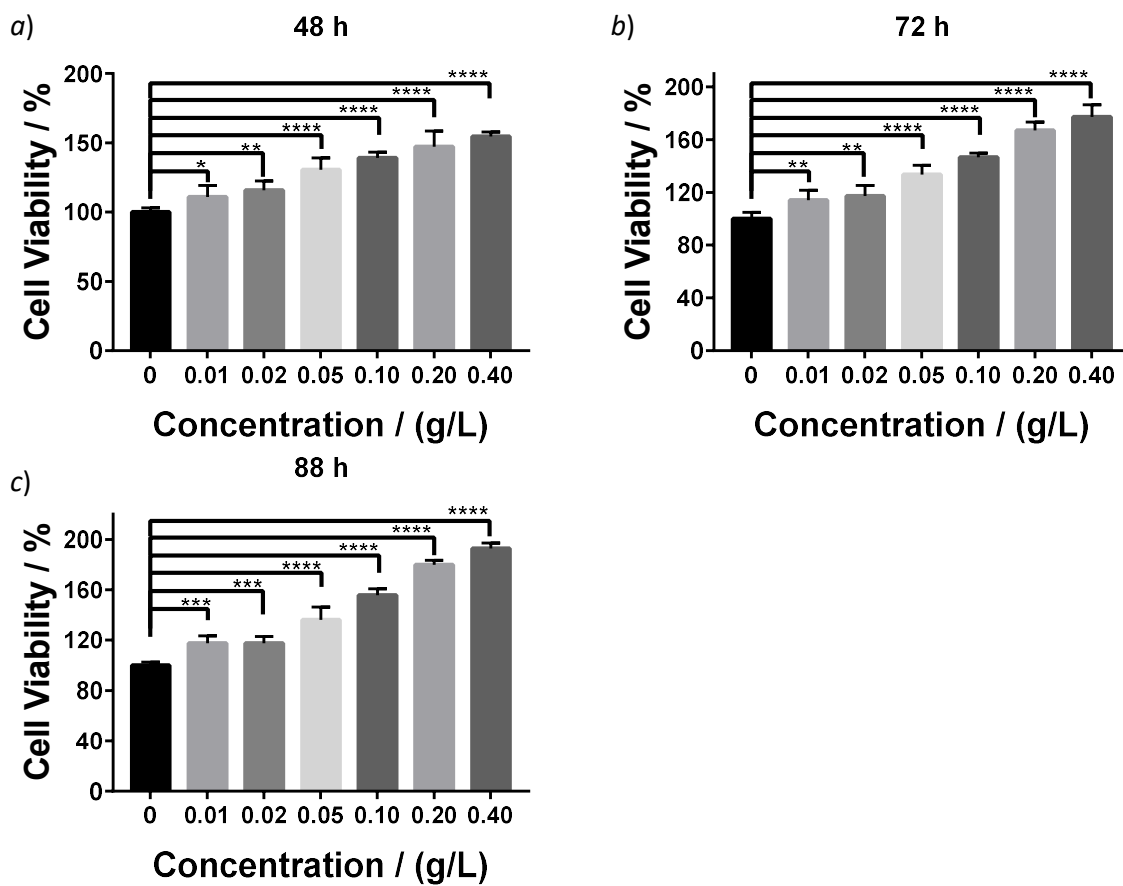


**Figure S25.** Cytotoxicity assay of HCECs against **BP1** vesicles after 20 min irradiation upon incubation for (a) 48, (b) 72, and (c) 88 h. Data are presented as mean  $\pm$  s.d. ( $n = 5$ );  $p$  values were calculated in comparison with the negative control. \* $p < 0.05$ ; \*\*  $p < 0.01$ ; \*\*\*  $p < 0.001$ ; \*\*\*\*  $p < 0.0001$ .

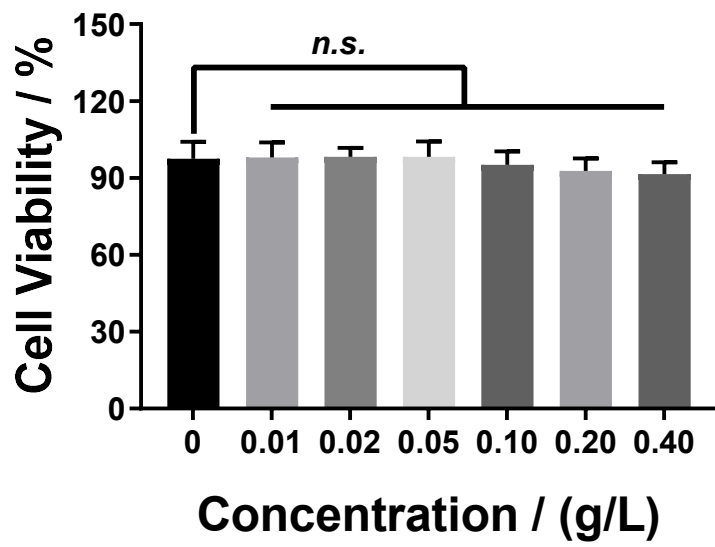


**Figure S26.** Cytotoxicity assay of HCECs against irradiated **BP1** vesicles. Data are presented as mean  $\pm$  s.d. ( $n = 5$ ); n.s., not significant.

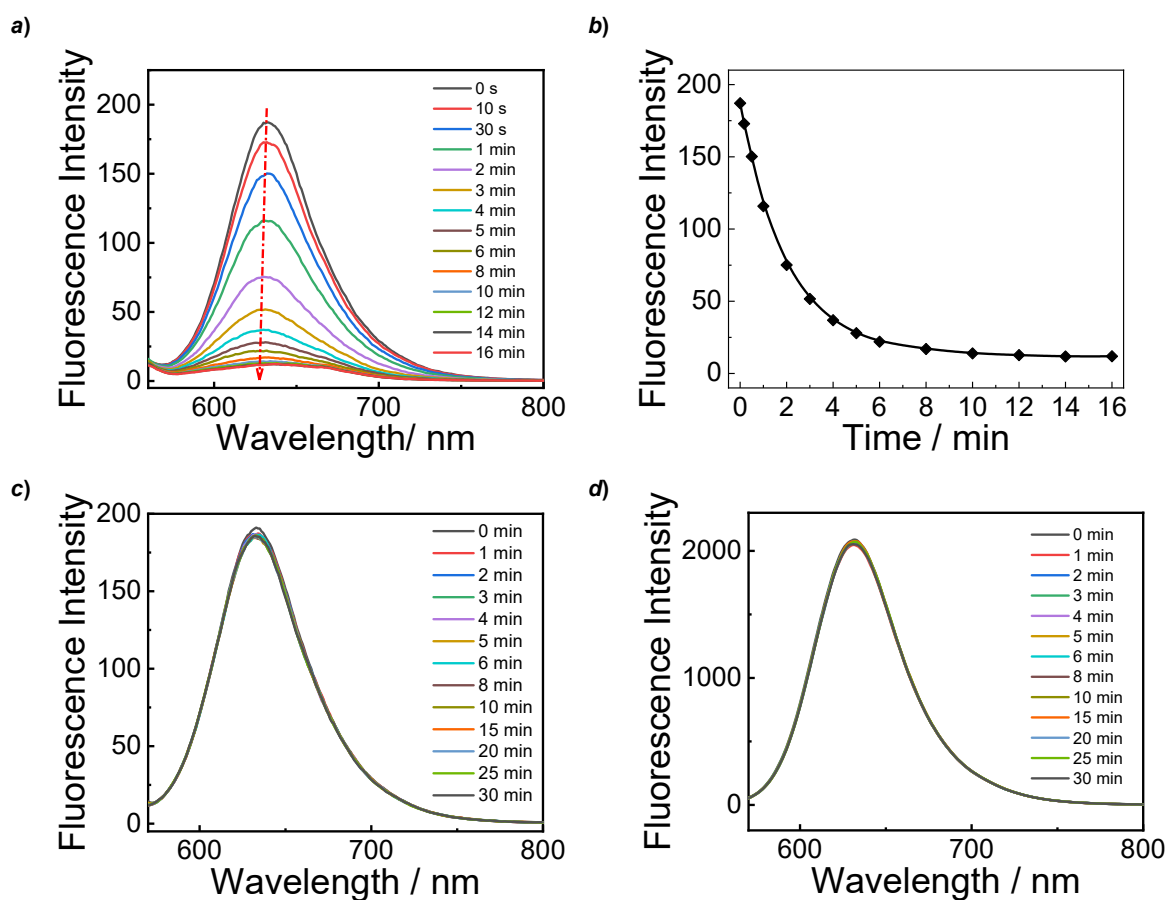


**Figure S27.** (a,c) Fluorescence emission spectra ( $\lambda_{\text{ex}} = 550 \text{ nm}$ ; slit widths: Ex. = 5 nm, Em. = 5 nm; Nile Red: 3.4  $\mu\text{M}$ ) and (b) fluorescence intensity changes at 633 nm of NR-loaded **BP1** vesicles (a) with and (c) without UV 365 nm irradiation (4  $\text{mW}/\text{cm}^2$ ). (d) Fluorescence emission spectra of NR (3.4  $\mu\text{M}$ ) in DMSO under UV 365 nm irradiation (4  $\text{mW}/\text{cm}^2$ ).

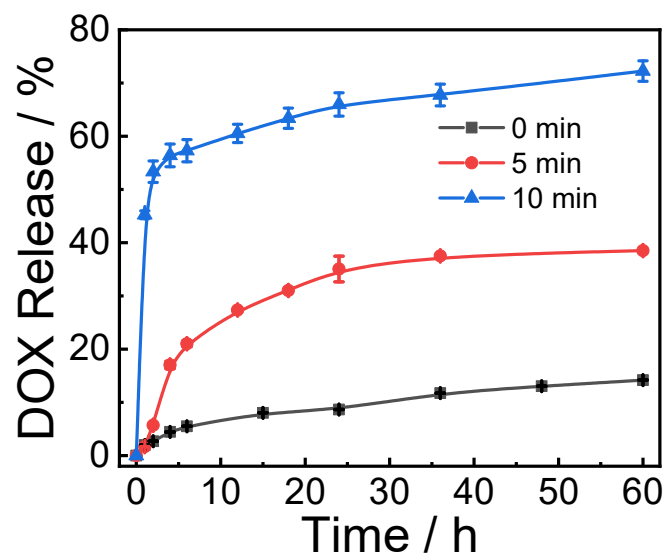


**Figure S28.** DOX release profiles from DOX-loaded **BP1** vesicles without or with light irradiation. Data are presented as mean  $\pm$  s.d. (n = 3).